NASA TECHNICAL NOTE

NASA TN D-4223

COMPARISON OF ABSOLUTE CALCULATED AND MEASURED GAMMA AND NEUTRON DOSES IN TUNGSTEN - WATER-MODERATED CRITICAL ASSEMBLY

by Paul G. Klann and Walter A. Paulson

Lewis Research Center
Cleveland, Ohio

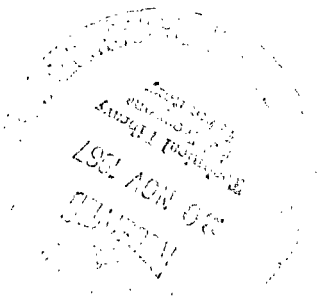

NATIONAL AERONAUTICS AND SPACE ADMINISTRATION • WASHINGTON, D. C. • NOVEMBER 1967

NASA TN D-4223

COMPARISON OF ABSOLUTE CALCULATED AND MEASURED GAMMA AND NEUTRON DOSES IN TUNGSTEN - WATER-MODERATED CRITICAL ASSEMBLY

By Paul G. Klann and Walter A. Paulson

Lewis Research Center
Cleveland, Ohio

NATIONAL AERONAUTICS AND SPACE ADMINISTRATION

For sale by the Clearinghouse for Federal Scientific and Technical Information
Springfield, Virginia 22151 – CFSTI price $3.00

CONTENTS

COMPARISON OF ABSOLUTE CALCULATED AND MEASURED GAMMA AND NEUTRON DOSES IN TUNGSTEN - WATER-MODERATED CRITICAL ASSEMBLY

by Paul G. Klann and Walter A. Paulson

Lewis Research Center

SUMMARY

The mixed gamma and neutron dose was measured at 60 locations within the Tungsten - Water-Moderated Reactor critical assembly. Graphite wall thimble ionization chambers filled with carbon dioxide and polyethylene wall chambers filled with ethylene were used. The chambers were absolutely calibrated in a bremsstrahlung beam against a secondary calibration standard and in a reactor against a water filled calorimeter. These calibrations were used to obtain gamma and neutron response coefficients for the chambers which permitted partitioning of the measured mixed radiation dose into a gamma dose and a neutron dose. The measured gamma doses were compared with an ATHENA Monte Carlo calculation. Good agreement was found for the 16 locations compared. The average deviation was 10 percent. In addition, the measured neutron doses were compared with a "first collision" calculation of the dose. The calculated neutron doses were uniformly low with an average deviation from the measurement of 18 percent.

INTRODUCTION

One of the important aspects of the Tungsten - Water-Moderated Rocket Reactor feasibility program was the specification of the gamma dose in the core water moderator and the core structure. A Monte Carlo gamma heating digital computer program, ATHENA, was developed by the United Nuclear Corporation for the NASA Lewis Research Center to calculate the rate of gamma energy deposition as a function of position in the core.

The accuracy of this program and the cross section data were checked by comparing gamma dose measurements conducted by the General Atomic Division of General Dynamics at the Tungsten - Water-Moderated Reactor (TWMR) critical facility with values calculated using ATHENA. The comparison of the calculated and measured gamma dose is given in this paper.

In addition, measurements were conducted by General Atomic in which the total dose from combined gamma and neutron radiation was determined at a number of locations within the critical assembly. The neutron dose results are compared with a refined first collision dose calculation in this paper.

GAMMA DOSE CALCULATIONS

Description of TWMR

Sixteen graphite wall, carbon dioxide filled thimble ionization chambers were used to measure the absolute gamma dose at 60 locations within the control tubes and the fuel

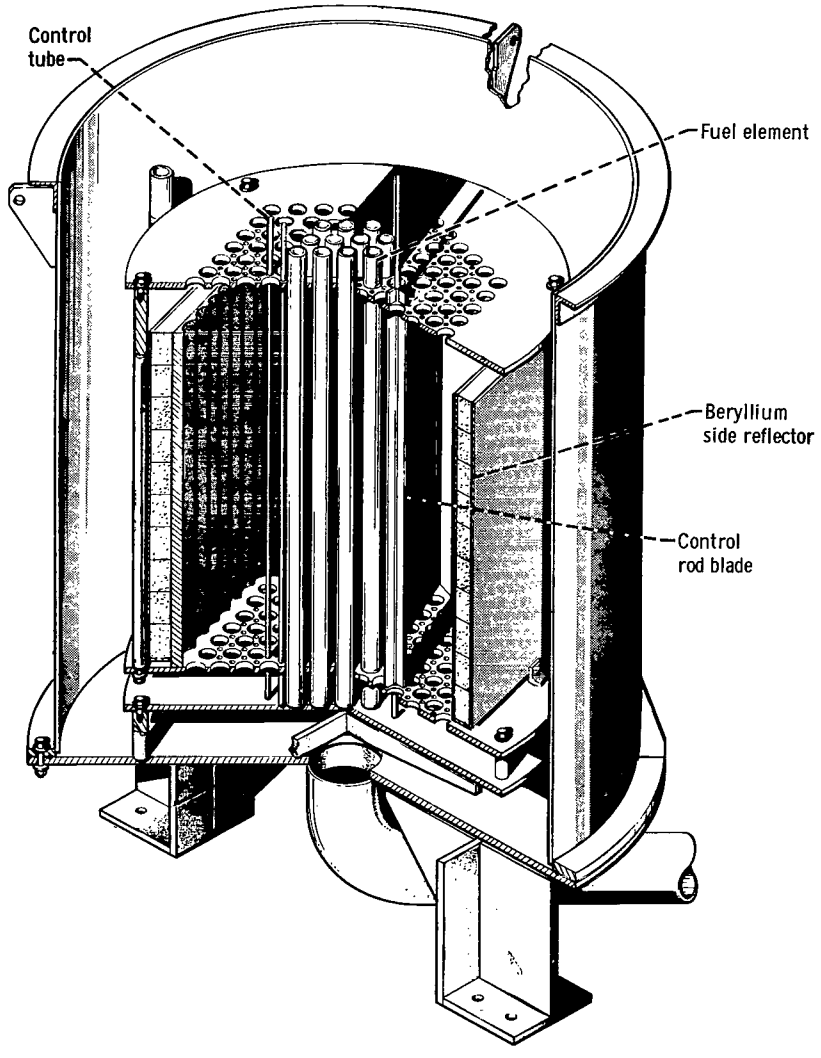

Figure 1. - Cross section of TWMR critical assembly.

elements of the Tungsten - Water-Moderated Reactor (TWMR) critical assembly (refs. 1 and 2). The TWMR critical assembly consisted of a hexagonal array of 121, 2.562-inch- (6.507 cm) diameter, 42.5-inch- (108 cm) long fuel elements spaced on a 3-inch (7.62 cm) triangular pitch in the water moderator. The core was reflected by beryllium backed with water on all sides with exception of the top 2.0-inch (5.08 cm) water reflector. A cross section of the core is shown on figure 1. The bottom beryllium reflector which was built up of $2\frac{7}{8}$ by $2\frac{7}{8}$ by 4 inches (7.30 by 7.30 by 10.16 cm) beryllium blocks placed in the space between the core support plate and the grid plate is not shown on this figure.

Each fuel element was composed of a series of concentric uranium 235, tungsten, aluminum, and uranium 238 rings within a hollow water-tight aluminum support tube. Figure 2 shows the cross section of the fuel element. Control tubes containing dilute solutions of cadmium nitrate were located in the triflutes between the fuel elements.

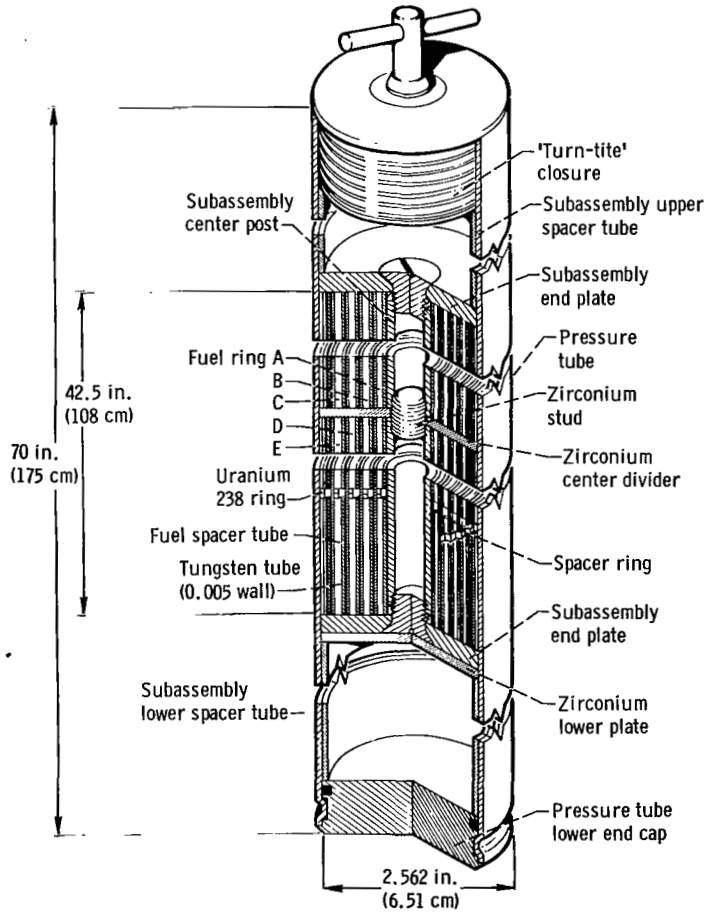

Figure 2. - TWMR fuel element.

Computer Program Description

The digital computer program, ATHENA, was used to calculate the gamma energy deposition rates at 16 of the graphite thimble ionization chamber locations. This computer program (ref. 3) employs Monte Carlo techniques to compute gamma-energy deposition rates as well as neutron and gamma fluxes in selected energy groups in complex, three-dimensional geometries. The option of representing a reactor by a symmetric 30° sector of the core with reflective boundaries at 0° and 30° makes this program especially efficient for calculations involving hexagonal-lattice reactors such as the TWMR critical assembly.

In ATHENA, the source neutrons and photons are selected based on detailed input-specified reactor geometry, region and importance sampling parameters, power pattern, and operating history. These are followed through the various interactions until the occurrence of capture, death by energy or region importance, or a degradation below an energy cutoff.

Calculational Model

The TWMR critical assembly was a heterogeneous core. Although the storage limitations of the digital computer did not permit detailed representation of each fuel cylinder in a stage, the essential heterogeneous nature of the core was retained in the calculational model. The main features of the core representation are as follows:

(1) The critical assembly was represented as a 30° sector of the hexagonal core with reflective boundaries at the 0° and 30° planes.

(2) Each fuel assembly was represented as a single right cylinder having the homogenized fuel element composition.

(3) The aluminum pressure tubes, water moderator, and bottom and side reflectors were represented explicitly.

(4) Each poison control tube was represented as a homogenized cylinder of aluminum plus cadmium control solution.

(5) Sixteen thimble ionization chambers were represented as right cylinders. Preliminary calculations showed that the small active volume of the chambers (about 1.8 cc) did not accumulate a good statistical sample of track lengths during the Monte Carlo calculation. To improve the statistics, the representation of the active volume was increased to 8.9 cubic centimeters by increasing the length. The experimentally measured axial distribution of absorbed dose is a smooth function of axial location; hence, the increased length of the active section of the chamber should not introduce a significant error in the calculated dose.

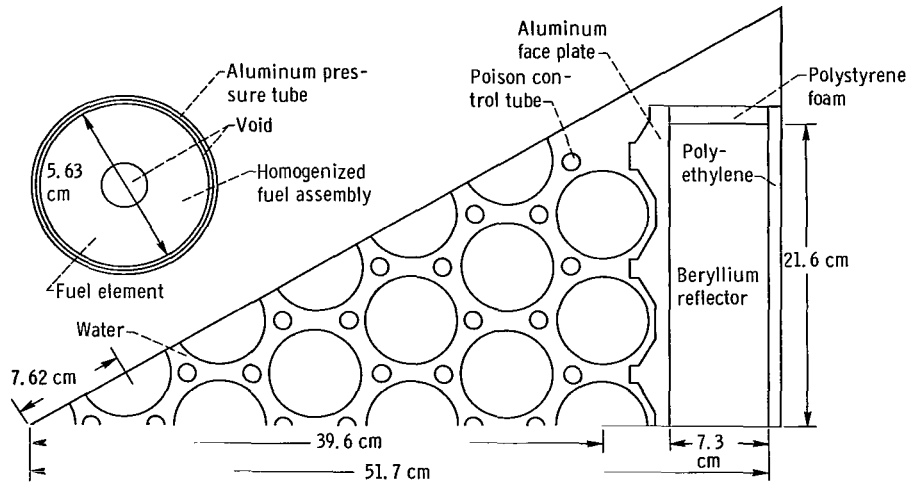

Figure 3. - Core calculational model.

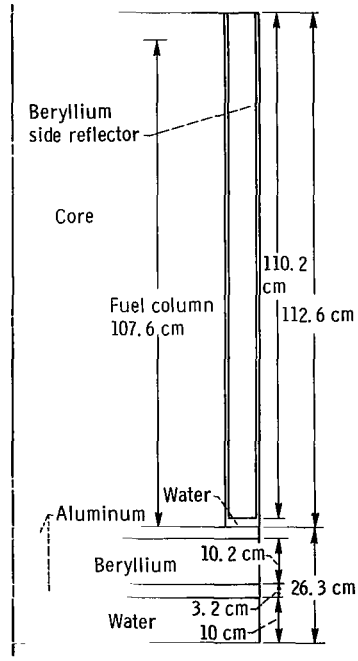

Figure 4. - Axial section of calculational model.

TABLE I. - COMPOSITION USED IN MONTE CARLO CALCULATIONS

	Isotope	Atom density	
		atom/barn-cm	atom/cc
Fuel element	Uranium 235	7.5992×10^{-4}	7.5992×10^{20}
	Uranium 238	3.1228×10^{-3}	3.1228×10^{21}
	Tungsten 182	5.1651×10^{-4}	5.1651×10^{20}
	Tungsten 183	2.8173×10^{-4}	2.8173×10^{20}
	Tungsten 184	5.9869×10^{-4}	5.9869×10^{20}
	Tungsten 186	5.5839×10^{-4}	5.5839×10^{20}
	Aluminum	2.8468×10^{-2}	2.8468×10^{22}
	Zirconium	1.2695×10^{-4}	1.2695×10^{20}
	Nickel	8.8814×10^{-5}	8.8814×10^{19}
Poison tube	Hydrogen	5.275×10^{-2}	5.275×10^{22}
	Oxygen	2.6375×10^{-2}	2.6375×10^{22}
	Aluminum	1.26×10^{-2}	1.26×10^{22}
	Cadmium	1.1282×10^{-4}	1.1282×10^{20}
Dosimeters	Carbon	6.1889×10^{-2}	6.1889×10^{22}
Polyethylene and polystyrene	Carbon	3.99×10^{-2}	3.99×10^{22}
	Hydrogen	7.98×10^{-2}	7.98×10^{22}
Water	Hydrogen	6.677×10^{-2}	6.677×10^{22}
	Oxygen	3.339×10^{-2}	3.339×10^{22}
Beryllium		1.228×10^{-1}	1.228×10^{23}
Aluminum		6.02×10^{-2}	6.02×10^{22}

Cross sections of the core calculational model are shown in figures 3 and 4. The atom densities used in the calculation are shown in table I.

Neutron and Primary Gamma Source Generation

The energy distribution of neutron source particles is based on a uranium 235 fission spectrum. The rejection technique used to select neutron energies from a portion of the fission spectrum as approximated by Cranberg is described in reference 3. For primary gamma-energy selection, the reactor operating history shown in figure 5 was used to obtain the delayed gamma contribution using built-in delayed gamma tables. These gamma tables are described in reference 4. The spatial distribution of both neutrons and primary gammas is determined based on the detailed axial and radial power

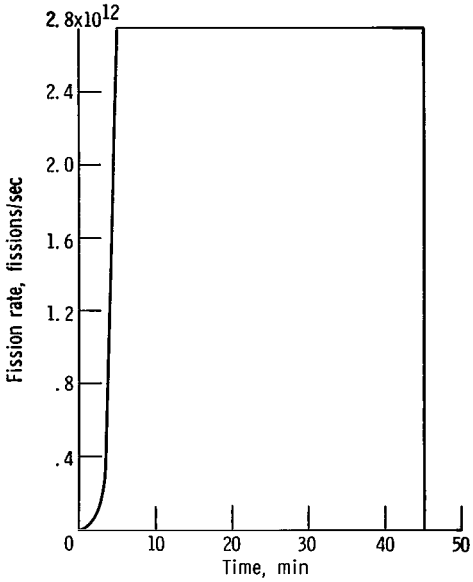

Figure 5. - Reactor operating history.

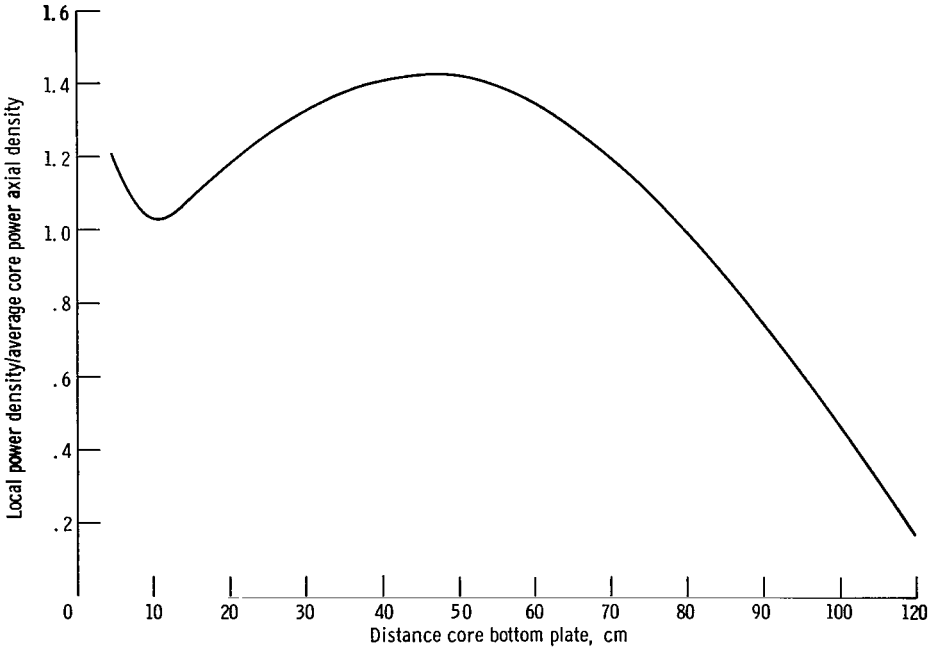

Figure 6. - Measured axial power distribution in center pull element of TWMR critical assembly.

TABLE II. - MEASURED RELATIVE POWER DENSITY AT MIDPLANE OF TWMR CRITICAL ASSEMBLY

Fuel element	Relative power density
K-1	0.744
J-1	.724
J-2	.712
J-3	.800
H-1	.771
H-2	.671
H-3	.781
H-4	.883
H-5	.949
G-2	.709
G-3	.733
G-4	.851
G-5	.938
G-6	.983
G-7	1.000

distributions (fig. 6 and table II) and fuel-element geometry. The angular distribution of the source particles was isotropic. Energy and region importance sampling were employed in the calculation. This technique modifies the a priori energy and spatial distribution and, in general, can result in a reduced variance of the Monte Carlo answers for a given number of source particles.

Secondary Gamma Source

Secondary gamma source particles were generated at the sites of neutron inelastic scattering and absorption. These events were recorded on an interaction tape during the neutron Monte Carlo calculation. The information recorded included the type of interaction, spatial location, energy of the neutron, and a number identifying the nuclide involved in the interaction. The interaction tape was then processed through the program, GASP, that generates the secondary gamma sources. The gamma production cross sections that were used are discussed in reference 4.

Monte Carlo Calculations

Eighty thousand primary gammas were tracked to determine this contribution to the total gamma dose. Gammas produced from tracking 8000 neutrons were used to determine the secondary gamma contribution to the total dose. A total of 144 tracking regions

were used in this calculation. The following table shows the time required on the IBM-7094 computer to perform the Monte Carlo Calculations:

Type of source	Computer time, min
Primary gamma	42.4
Neutron	51.3
Secondary gamma	41.3

The cross section data used in ATHENA were specified in 81 equal lethargy intervals from 0.037 eV to 18.02 MeV for neutrons and from 10 keV to 10 MeV for photons.

Results of Calculation

The total dose calculated for the 16 chambers are shown in table III. The dose is based on the calculated energy deposition rates which were assumed to be constant over

TABLE III. - COMPARISON OF CALCULATED AND MEASURED GAMMA DOSE

Chamber location (a)	Distance from core bottom plate to center of chamber, cm	Chamber	Calculated gamma dose in graphite		Measured gamma dose in graphite		Percent deviation
			rads	J/kg	rads	J/kg	
G-4	84.7	C-7	680± 72	6.8 ±0.72	883	8.83	-23
G-4	62.1	C-6	1170± 94	11.7 ± .94	1253	12.53	+7
G-4	37.1	C-1	1153± 92	11.53± .92	1207	12.07	-4
G-4	9.5	C-5	975± 79	9.75± .79	880	8.80	+11
G-2	62.1	C-1	987±104	9.87±1.04	839	8.39	+18
G-2	37.1	C-11	744± 81	7.44± .81	881	8.81	-15
K-1	37.1	C-11	831± 97	8.31± .97	850	8.50	-2
g-10	84.7	C-13	849± 89	8.49± .89	870	8.70	-2
g-10	37.1	C-7	1130± 93	11.3 ± .93	1279	12.79	-11
g-10	6.6	C-10	796± 86	7.96± .86	828	8.28	-4
g-8	37.1	C-6	1290±109	12.9 ±1.09	1201	12.01	+7
g-6	105.5	C-13	301± 44	3.01± .44	250	2.50	+20
g-6	62.1	C-12	960± 78	9.6 ± .78	989	9.89	-3
g-6	37.1	C-5	1143± 94	11.43± .94	1055	10.55	+8
g-6	6.6	C-3	648± 74	6.48± .74	723	7.23	+10
g-4	37.1	C-1A	875± 84	8.75± .84	804	8.04	+9

[a]See fig. 10.

the 40-minute reactor operating time. A comparison between the calculated and the corresponding experimentally measured values is given. The experimental measurements are discussed in the next section.

GAMMA DOSE MEASUREMENTS

Description of Graphite Ionization Chambers

The graphite wall, carbon dioxide filled chambers were 0.490 inch (1.24 cm) in diameter and 1.90 inch (4.83 cm) long and could be inserted within the control tubes or within the center post of the fuel element. The graphite chamber is shown in figure 7.

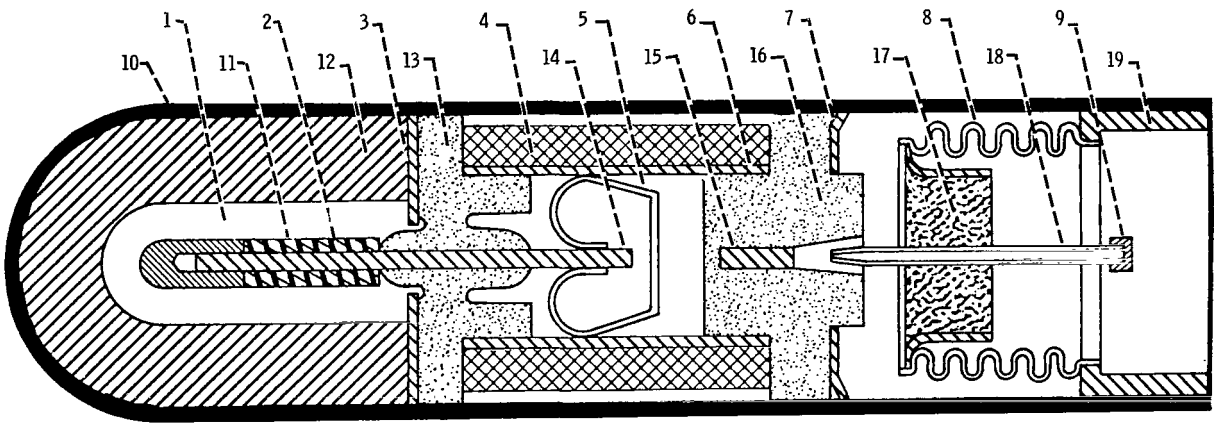

1, Ionizable volume - 0.176 cm^3 (carbon dioxide gas)
2, Carbon electrode sheath (0.064 in. diam)
3, Aluminum shield (0.015 in. thick)
4, Condenser (6000 (pF))
5, Electrode clip
6, Aluminum condenser core
7, Retainer ring
8, Bellows assembly
9, End cap
10, Aluminum shell 1.900 in. long - 490 in. diam - 0.015 in. wall
11, Aluminum electrode cap
12, Carbon chamber (0.134 in. wall)
13, Electrode insulator
14, Aluminum electrode
15, Electrode contact bar
16, Condenser insulator
17, Glass seal
18, Contact pin
19, End sleeve

Figure 7. - 2500 rad graphite ionization chamber.

These chambers were hermetically sealed and were charged and read by pushing the contact pin thereby stretching the bellows at the end of the chamber until electrical contact is made with the inner electrode. The electrical leakage of the chambers was about 2 percent of full scale per day.

Since the diameter of the chambers was restricted to permit insertion into the poison tubes, the areal density of the graphite walls was limited to 0.544 gram per square centimeter. This thickness exceeds the range of a 1.25 MeV electron and, therefore, corresponds to charged particle equilibrium for at least a 1.5 MeV photon. Actually,

charged-particle equilibrium is generally achieved at a wall thickness considerably less than the range of the highest energy secondary electron produced by the primary photon interaction. The effective wall thickness is greater since the chambers are surrounded by aluminum when positioned in the fuel elements and by aluminum and water when positioned within the poison tubes. If only aluminum surrounded the ionizable volume, then the measured dose would be 4 percent less than for carbon. If only water surrounded the ionizable volume, then the measured dose would be 11 percent greater. The largest error would therefore occur when the graphite wall chambers are surrounded by water. In this case, the total error caused by the walls not being in charged particle equilibrium for photons greater than 1.5 MeV should be no more than 4 percent.

The graphite ionization chambers have a small inherent sensitivity to fast neutrons caused by carbon recoils. Since the carbon recoil atoms generated in the walls would be largely absorbed in the walls, the neutron response of the chamber would be largely that of the recoils in the carbon dioxide gas. The experimental results were analytically corrected for the neutron recoils in the carbon dioxide gas as discussed in the section Correction for the Neutron Sensitivity of Graphite Chambers.

TABLE IV. - LANDSVERK ELECTROMETER

COMPANY CALIBRATION CERTIFICATE[a]

[Range, 2500 rads (25 J/kg) (carbon).]

Serial number	Response of graphite dosimeters			
	Cobalt 60 gamma-ray source	Gamma energy levels		
		120 keV	80 keV	46 keV
C1	76.2	81.1	89.6	46.6
C2	78.4	82.5	90.3	44.3
C3	94.4	93.5	88.8	51.2
C4	74.0	73.3	66.9	35.9
C5	86.0	84.8	89.6	43.7
C6	84.4	83.6	77.7	42.9
C7	87.0	86.0	81.6	46.0
C8	84.8	84.2	76.8	42.0
C9	80.0	79.4	82.7	40.0
C10	90.2	89.3	81.9	43.5
C11	85.6	84.8	80.3	41.7
C12	85.2	84.4	77.3	41.7
C13	107.2	106.2	96.0	49.2
C14	85.8	85.0	81.4	43.2
C15	84.4	83.4	75.5	42.4
C16	94.0	93.1	85.4	44.3

[a]Dated Nov. 1965.

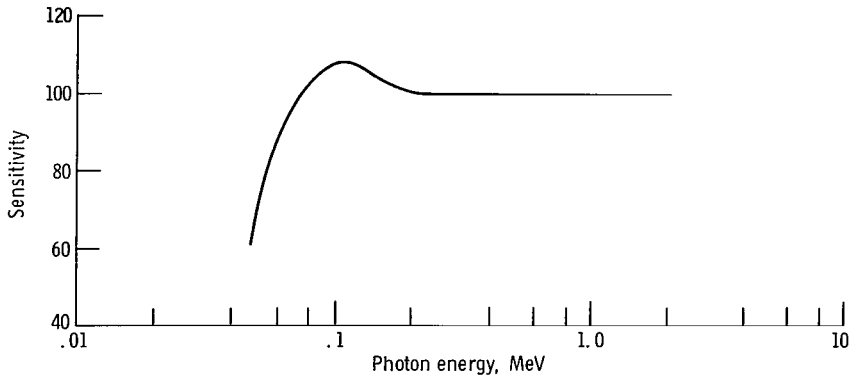

Figure 8. - Typical 2500 rad graphite ionization chamber response curve.

The energy response for each graphite chamber obtained with a cobalt 60 source and with X-rays are given in table IV. Figure 8 shows a typical energy response curve for the graphite chamber.

Absolute Calibration of Graphite Ionization Chambers

The graphite chambers were calibrated at General Atomic by comparison with a standard thimble chamber in a bremsstrahlung beam resulting from 7 MeV Linac generated electrons impinging on a thick fansteel (89 percent tungsten, 7 percent nickel, and 4 percent copper) target. The bremsstrahlung beam approximated a fission spectrum. Since all the photons were below the (γ, n) threshold of the target elements, the beam contained no neutrons.

The bremsstrahlung beam was directed to the center of a 4-inch- (10.16 cm) thick, 12-inch- (30.48 cm) diameter graphite disk shown in figure 9 containing eighteen 1/2-inch- (1.27 cm) diameter, $2\frac{3}{4}$-inch- (6.985 cm) deep holes drilled on a 9-inch (22.86 cm) diameter. All the graphite chambers were inserted into these holes and the graphite disk rotated at 2 revolutions per minute during the calibration. The thickness of the graphite between the ionization chamber and the front surface of the graphite was $1\frac{1}{4}$ inches (3.175 cm) and thus slightly greater than the range of a 7 MeV electron; therefore, particle equilibrium is established for photons at or below 7 MeV.

All the graphite ionization chambers were intercalibrated on a relative basis during a single measurement. However, since the range of the graphite ionization chambers was several thousand roentgens and the standard calibration chamber was limited to 25 roentgens (2.09 J/kg-air), a photodiode-plastic fluor detector (ref. 5) was used to monitor the measurements during the intercalibration. The instantaneous dose rate was 1×10^3 roentgens per second (8.38 J kg^{-1} (air) sec^{-1})) using a pulse length of 4.5 microseconds and a pulse rate of 180 per second from the Linac. A 30-minute run resulted in about a half-

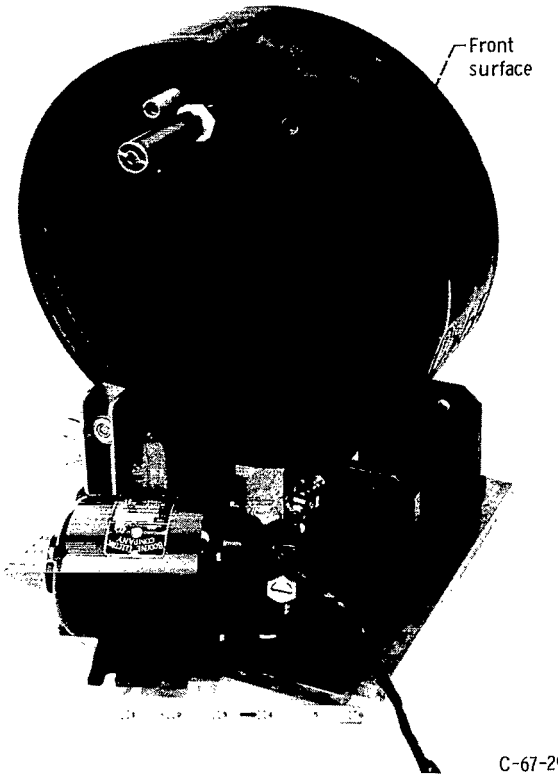

Figure 9. - Ionization chamber calibration apparatus.

scale reading on the graphite chambers which corresponded to about 2600 roentgens (21.7 J/kg-air).

The standard calibration chamber was then inserted in an especially enlarged hole in the graphite disk and irradiated together with the photodiode plastic fluor detector until an approximate midscale reading on the standard calibration chamber was obtained. The standard calibration chamber behaved as an air-equivalent dosimeter from 20 keV to 7 MeV. The exposure level of the standard chamber was compared with the reading on the photodiode-plastic fluor detector several times during this irradiation to obtain an average value. The maximum deviation between the several measurements of the average was found to be less than 1 percent.

The ratio of the photodiode plastic fluor detector reading obtained for the calibration of the graphite chamber to the reading obtained for the intercomparison with the standard chamber was multiplied by the standard chamber reading in roentgens (or J/kg-air) and then converted to rads (or J/kg) using the conversion factor 1 roentgen = 0.87 rad (0.00838 J/kg-air = 0.0087 J/kg-graphite).

The resulting rad (J/kg) value was then divided by the decimal fraction of full-scale read on each of the graphite chambers during the intercomparison to obtain the full-scale reading in rads (J/kg) dose to graphite for each individual chamber. The results of the absolute calibration of the graphite chambers are tabulated in table V.

TABLE V. - DOSIMETER CALIBRATION USING 7.0 MeV BREMSSTRAHLUNG RADIATION

(a) Graphite ionization chamber; gamma response coefficient, 0.9009

Ionization chamber number	Chamber reading, percent of full scale			Value obtained from standard calibration chamber		Average corrected chamber reading, full scale value	
	Uncorrected reading	Drift correction	Corrected reading	rads	J/kg	rads	J/kg
C-1	56.4	0	56.4	2300	23.00	4039	40.39
C-1	51.0		51.0	2030	20.30		
C-2	63.5		63.5	2300	23.00	3622	36.22
C-3	63.5		63.5	2300	23.00	3573	35.73
C-3	57.6		57.6	2030	20.30		
C-1A	63.2		63.2	2300	23.00	3639	36.39
C-5	57.9		57.9	2300	23.00	3941	39.41
C-5	51.9		51.9	2030	20.30		
C-6	56.0		56.0	2300	23.00	4107	41.07
C-7	58.0		58.0	2300	23.00	3928	39.28
C-7	52.2		52.2	2030	20.30		
C-8	63.2		63.2	2300	23.00	3639	36.39
C-9	56.8		56.8	2300	23.00	4038	40.38
C-9	50.4		50.4	2030	20.30		
C-10	61.4		61.4	2300	23.00	3746	37.46
C-11	56.2		56.2	2300	23.00	4089	40.89
C-11	49.7		49.7	2030	20.30		
C-12	60.9		60.9	2300	23.00	3777	37.77
C-13	71.5		71.5	2300	23.00	3194	31.94
C-13	64.0		64.0	2030	20.30		
C-14	58.9		58.9	2300	23.00	3886	38.86
C-14	52.5		52.5	2030	20.30		
C-15	61.8	3.7	58.1	2300	23.00	3959	39.59
C-16	65.2	.6	64.6	2300	23.00	3560	35.60

(b) Polyethylene ionization chamber; zero drift correction

Ionization chamber number	Chamber reading, percent of full scale		Value obtained from standard calibration chamber		Average corrected chamber reading, full scale value		Gamma response coefficient, ϵ
	Uncorrected reading	Corrected reading	rads	J/kg	rads	J/kg	
P-1	26.9	26.9	2630	26.30	12 860	128.60	1.19
P-1	25.0	25.0	2320	23.20	12 860	128.60	1.25
P-2	22.2	22.2			14 920	149.20	1.29
P-3	22.3	22.3			14 090	140.90	1.22
P-4	23.6	23.6			14 190	141.90	1.30
P-5	22.0	22.0			14 220	142.20	1.21
P-6	25.5	25.5			11 400	114.00	[a]1.13
P-7	26.8	26.8			12 150	121.50	1.26
P-8	28.0	28.0			12 360	123.60	1.35
P-9	22.0	22.0			14 620	146.20	[a]1.64
Average							1.26

[a]Not used in average.

The possible individual errors in this calibration are

(1) ±2 percent in the average energy to produce an ion pair in air for the roentgen to rad (J/kg-air to J/kg-graphite) conversion

(2) ±2 percent in the reading of the graphite chambers

(3) ±2 percent in the reading of the standard calibration chamber

(4) ±1 percent in the value used to convert the standard calibration chamber reading to the intercalibration run for the graphite chambers.

(5) ±2 percent in the photodiode-plastic fluor detector readings

(6) ±2 percent in the absolute roentgen value of the standard calibration chamber

It is estimated that this absolute calibration procedure gives the true absorbed gamma dose within ±5 percent.

Positioning of Graphite Chambers in TWMR Critical Assembly

As can be seen in figure 1, the TWMR critical assembly has a regular hexagonal cross section. Therefore, measurements in only one twelfth sector were required to obtain to an overall description of the gamma dose in the core. The positioning of the chambers is schematically shown in figure 10. The chambers were positioned above and below the zirconium stud using 3/8-inch- (0.952-cm) diameter, 0.060-inch- (0.1524-cm) wall-thickness aluminum tube spacers. In the control tubes, 5/16-inch- (0.7938-cm) diameter, 0.060-inch- (0.1524-cm) wall-thickness tube spacers were used and the space between the chambers filled with the cadmium nitrate solution. Also shown in figure 10 are the locations of the polyethylene wall, ethylene filled ionization chambers used in connection with the total neutron plus gamma dose measurements described later.

The measurements were made in four runs, each run employing 16 graphite wall and 9 polyethylene-wall ionization chambers. For each run the same graphite-wall chamber was placed in the G-7 (center) fuel element and the same polyethylene-wall chamber in the g-16 control tube to monitor the relative power level between runs. The relative variation in the integrated dose and therefore the power level from run to run as indicated by the monitor ionization chambers was within 3 percent.

Irradiation of Chambers in TWMR

Each of the four irradiating runs lasted 40 minutes at full power. The reactor was brought to full power on a 30-second period.

A measurement of the gamma time history was made for each of the four reactor runs using a gamma scintillation detector which discriminated against fast neutrons.

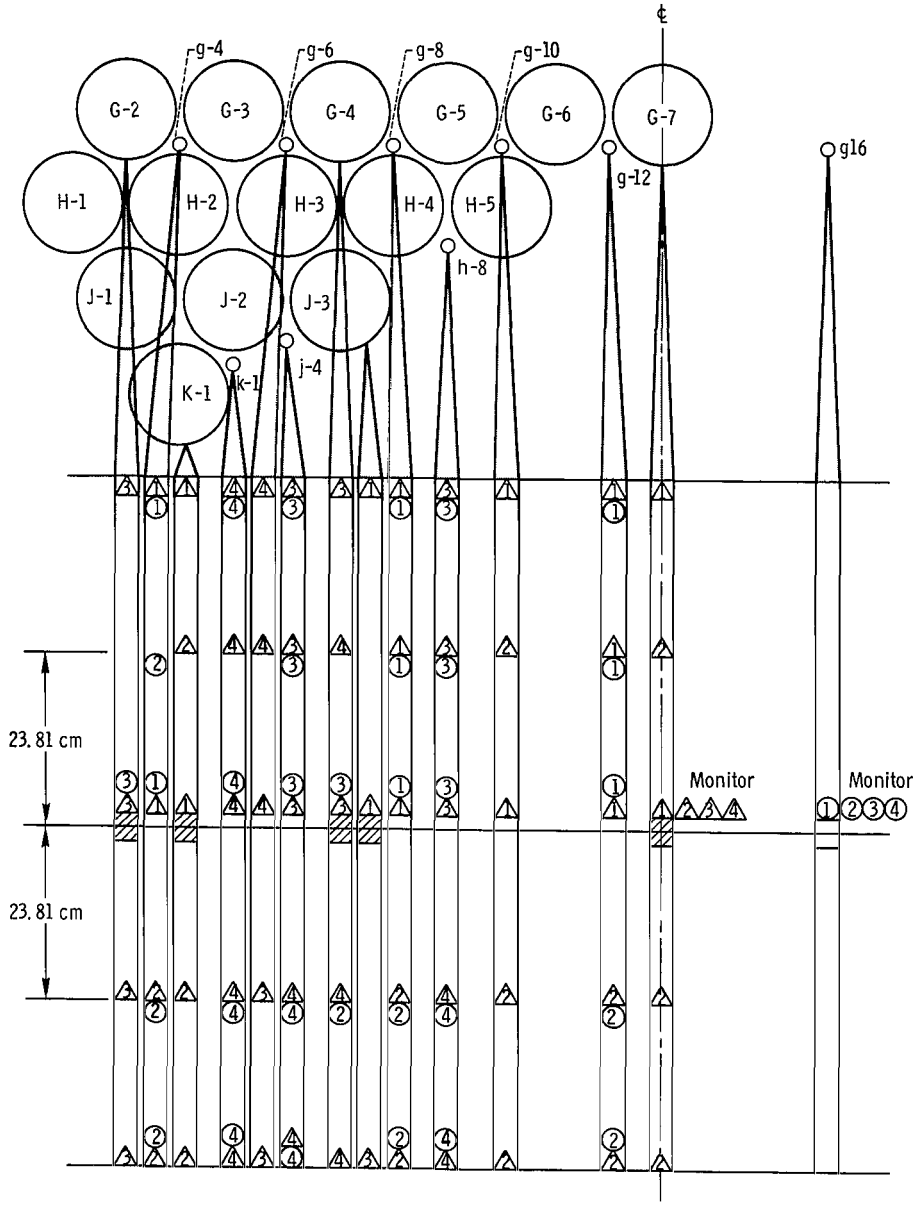

Run	Number of graphite chambers in -	
	Fuel element	Poison tube
1	6	10
2	7	9
3	8	8
4	4	12

△

Run	Number of polyethylene chambers in -	
	Fuel element	Poison tube
1	---	9
2	1	8
3	2	7
4	---	9

○

Figure 10. - Placement of ionization chamber in the TWMR critical assembly.

This detector was located about 2 feet (61 cm) above the beryllium reflector at the edge of the core and the relative gamma intensity measured as a function of time for each of the reactor runs. The relative gamma intensity as a function of time for the four runs are shown in figure 11.

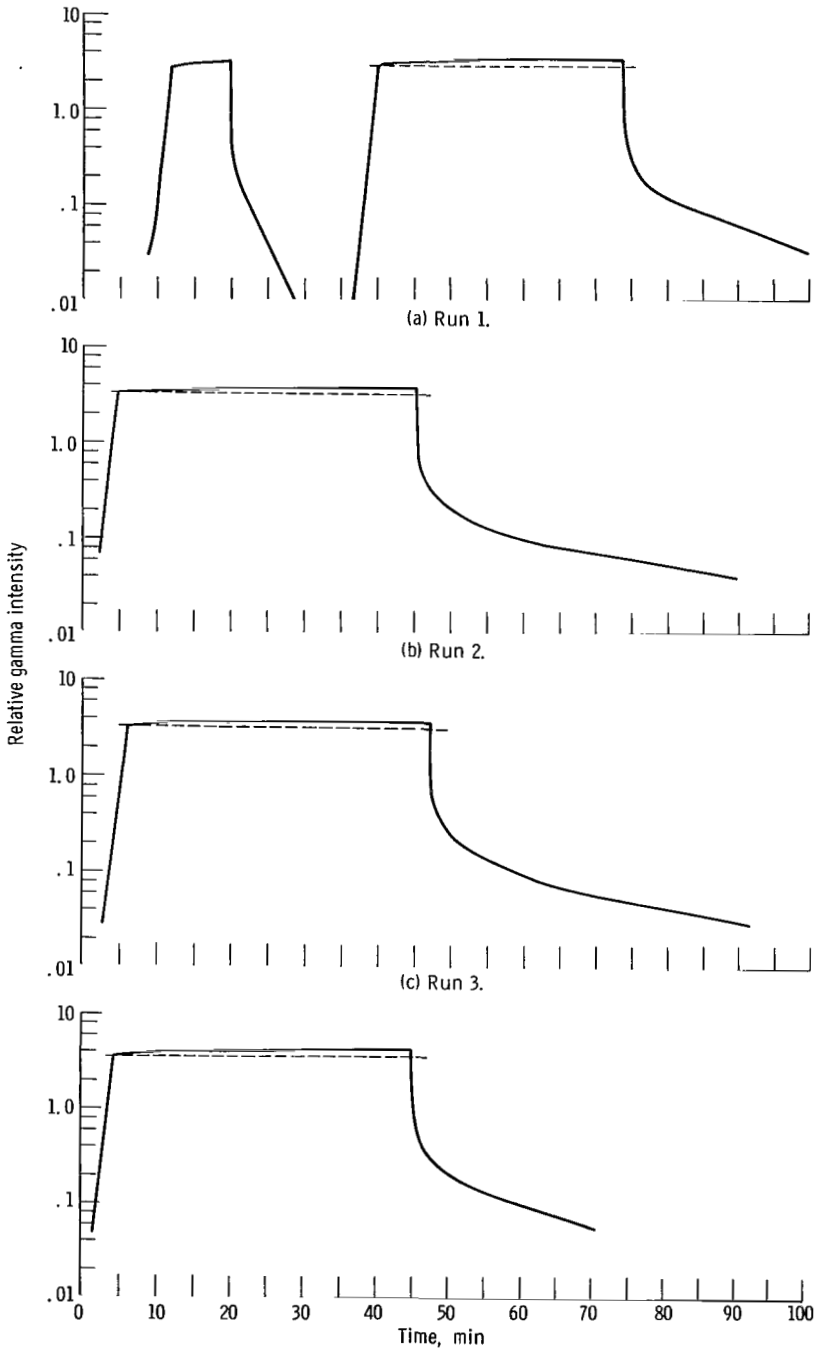

Figure 11. - Gamma intensity time history.

Correction for Neutron Sensitivity of Graphite Chambers

As has been noted before, the graphite chambers have an inherent sensitivity to fast neutrons because of the ionization caused by recoiling carbon and oxygen atoms in the carbon dioxide fill gas and, to a smaller extent, because of recoiling carbon atoms emitted from the graphite wall. The second effect is considered to be negligible since the recoil atoms would be largely absorbed in the walls.

The reading (in rads (J/kg)) of the graphite chamber R_C resulting from irradiation in the TWMR critical assembly therefore consists of the dose KG in the graphite wall deposited by the photons plus the dose νN in the carbon dioxide gas deposited by the fast neutrons.

$$R_C = KG + \nu N \tag{1}$$

(Symbols are defined in the appendix) where G is the gamma dose (rads or J/kg) deposited in water at the position of the graphite chamber, K is the ratio of gamma dose (rads or J/kg) in graphite to the gamma dose (rads or J/kg) in water. (The value of K is 0.9009 (ref. 2)), N is the fast neutron dose (rads or J/kg) deposited to water at the position of the graphite chamber, and ν is the ratio of the fast neutron dose in carbon dioxide to the fast neutron dose in water. The value of ν was calculated as outlined later.

When equation (1) is solved for the corrected gamma dose KG, and the ratio G/(G + N) is replaced by the equivalent spectrum index S, equation (2) results.

$$KG = R_C \left[\frac{1}{1 + \frac{\nu}{K}\left(\frac{1}{S} - 1\right)} \right] \tag{2}$$

This equation is used to correct the measured graphite chamber reading R_C to the true rad (J/kg) dose deposited in graphite KG.

The ratio S was measured in 23 locations in the TWMR core and an average value for $\bar{S}$ of 0.29±0.03 obtained. The construction and calibration of the polyethylene chambers and the techniques used to obtain the ratio $\bar{S}$ for the TWMR core are discussed in the section TOTAL RADIATION DOSE MEASUREMENTS.

The value of ν was calculated from the following considerations. Fast neutrons colliding with low-mass atoms impart appreciable energy to the recoiling atom since the average fraction f of energy imparted per elastic collision (assuming isotropic scattering in the center-of-mass system) is $2M/(M + 1)^2$ where M is the atomic mass of the recoil atom. The energy imparted to 1 gram of atoms D for a neutron flux per energy

initial ΔE centered about the energy E is

$$D = \mathcal{N}\sigma_s f E \varphi(E)\Delta E \tag{3}$$

where $\mathcal{N}$ is the atomic number density in atoms/gram, σ_s is the elastic scattering cross section, and $\varphi(E)\Delta E$ is the flux in the interval ΔE centered about the energy E. Thus, the total dose to 1 gram of material per unit time from fast neutrons is

$$D_{tot} = \int_{E_L}^{\infty} \mathcal{N}\sigma_s f E \varphi(E) dE \tag{4}$$

where E_L is the lower limit of the fast neutron range. Since the chamber reading is proportional to the ionization caused by the recoiling nuclei, the lower limit of the fast neutron range is assumed to occur at the energy at which the recoiling atom moves so slowly that ionization of the material becomes improbable. The lower limit is believed to be 10 keV for the proton recoils (ref. 6) resulting from the bombardment of hydrogen by 20-keV neutrons. The equivalent lower limits of the fast neutron range of 860 keV for carbon and 1.5 MeV for oxygen are obtained by scaling up the hydrogen values considering the lower average energy transfer and higher energy required for equal speeds for these atoms.

Thus, the expression for ν, the ratio of the neutron dose per gram of carbon dioxide to the neutron dose per gram of water, is

$$\nu = \frac{\sum_{i=1}^{29} \mathcal{N}_C \sigma_{si}^{C} f_C E_i \varphi_i \Delta U_i + \sum_{j=1}^{23} \mathcal{N}_O \sigma_{sj}^{O} f_O E_j \varphi_j \Delta U_j}{\sum_{k=1}^{56} \mathcal{N}_H \sigma_{sk}^{H} f_H E_k \varphi_k \Delta U_k + \sum_{l=1}^{23} \mathcal{N}_O \sigma_{sl}^{O} f E_l \varphi_l \Delta U_l} \tag{5}$$

where C, O, and H are carbon, oxygen, and hydrogen, respectively. The integral of equation (4) has been replaced by a summation over the GAM II fine-group structure. The GAM II code (ref. 7) was used to supply fine-group elastic scattering cross section σ_{si} and fine-group flux values φ_i starting at 14.9 MeV for the calculation. The ΔU_i are the lethargy widths for the fine groups ($\Delta U = 0.1$ from 14.9 MeV to 86.5 keV; $\Delta U = 0.25$ from 86.5 keV to E_L), and E_i is the energy at the midpoint of each interval.

The shape of the neutron spectrum $\varphi(U)$ computed by the GAM II code is dependent on the input buckling. The fast group buckling obtained from a one-dimensional transport

theory TDSN (ref. 8) calculation of the TWMR critical assembly was used in GAM II. The buckling dependent, zero dimensional GAM II computed neutron spectrum is compared with the ATHENA computed three-dimensional neutron spectrum in the center water region in figure 12. Good agreement is noted both in the spectrum and in the magnitude of the flux.

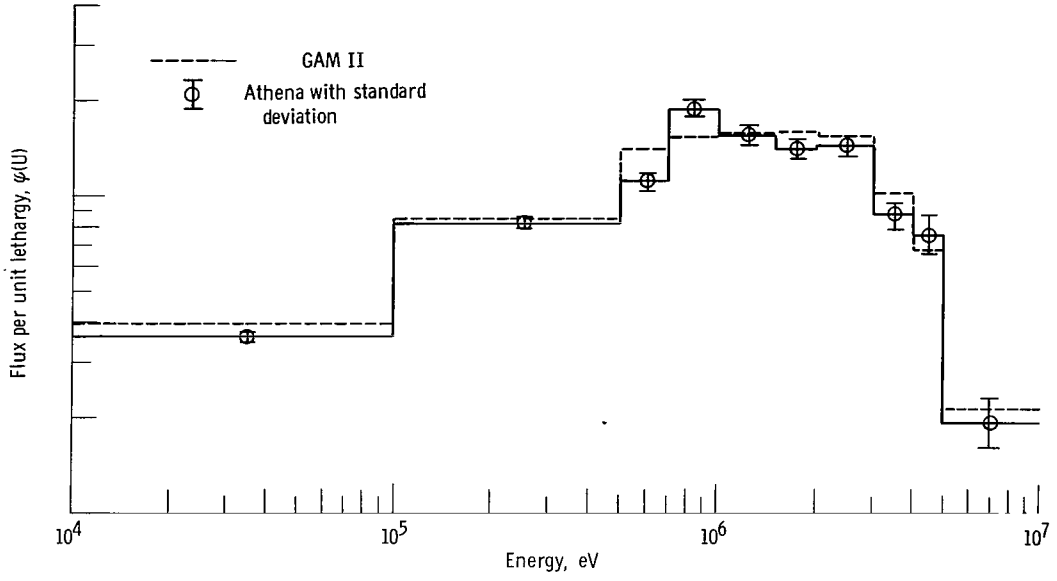

Figure 12. - Comparison of GAM II and Athena calculated neutron spectrum in central water region of TWMR critical aseembly.

The value computed for ν using equation (5) was 0.0634±0.0187. The error assigned to ν reflects the lack of reliable data on the lower energy limit of the fast neutron range for hydrogen, carbon, and oxygen and to a much lesser extent (because the flux appears in both the numerator and denominator of eq. (5)) on the uncertainty in buckling value used in the GAM II spectrum calculation. The magnitude of the error was obtained by recalculating ν using a GAM II spectrum in which the buckling was reduced by 30 percent to the overall epithermal buckling value used in neutronic calculations for this core. The lower limit of the fast neutron range for all the elements was taken to be 19.3 keV. The buckling change has only a few percent effect on ν, while the reduced lower limit of the fast neutron range tends to greatly increase ν. The recalculated value for ν was 0.1008. This value is considered to be the upper limit of the ratio of neutron dose in carbon dioxide to the neutron dose in water. Since the uncertainty is one-sided about ν, one-half of this difference in ν was assigned as the error in ν. It must be noted that although the error assigned to ν is nearly 30 percent, the resulting error in KG, the gamma dose in graphite as obtained by equation (2), is only 4 percent.

Results of Gamma Dose Measurements

The absolute gamma dose in the graphite KG was obtained from the graphite chamber readings R_C using equation (2). Substitution of the parameters ν, K, and $\bar{S}$ leads to equation (6).

$$KG = R_C\left[\frac{1}{1 + \frac{\nu}{K}\left(\frac{1}{\bar{S}} - 1\right)}\right] = R_C\left[\frac{1}{1 + \frac{0.06341}{0.9009}\left(\frac{1}{0.29} - 1\right)}\right] = 0.853\ R_C \tag{6}$$

The data and results are listed in tables III and VI.

Error Analysis of Gamma Dose Measurements

The relation between the parameters in equation (2) was used to propagate the uncertainties in ν, $\bar{S}$, and R_C to determine the resulting error in the measured gamma dose to graphite.

$$\frac{\Delta(KG)}{(KG)} = \pm\sqrt{\left(\frac{\Delta R_C}{R_C}\right)^2 + 0.0216\left(\frac{\Delta\nu}{\nu}\right)^2 + 0.0428\left(\frac{\Delta\bar{S}}{\bar{S}}\right)^2} \tag{7}$$

The uncertainty in R_C consists of the ±5 percent uncertainty in the calibration of the graphite chambers discussed earlier, a ±2 percent uncertainty in reading the graphite chamber, a ±3 percent uncertainty in the time at which the reactor was at power, and a ±7 percent uncertainty in the measurement power level of the reactor which is discussed in the section Measurement of Absolute Power Level. Thus, the total uncertainty in R_C is ±9 percent. If the error in measurement of the power level is neglected, the uncertainty is ±6 percent. As was discussed earlier, an uncertainty of ±30 percent was assigned to ν, and an uncertainty of ±10 percent resulted from the measurements of $\bar{S}$ in the TWMR. Thus, the total error in the value of KG as given by equation (7) is ±10 percent.

TABLE VI. - RESULTS OF GRAPHITE IONIZATION CHAMBER MEASUREMENTS IN TWMR CRITICAL ASSEMBLY

Control tube or fuel element	Distance from core bottom plate to center of chamber, cm	Chamber number	Chamber reading with run normalization included, R_C		Absorbed gamma dose in graphite, KG[a]	
			rads	J/kg	rads	J/kg
G-2	9.4	C-16	698	6.98	594	5.94
	37.1	C-11	1035	10.35	881	8.81
	62.1	C-1	986	9.86	839	8.39
	105.1	C-12	362	3.62	309	3.09
G-4	9.5	C-5	1034	10.34	880	8.80
	37.1	C-1	1418	14.18	1207	12.07
	62.1	C-6	1472	14.72	1253	12.53
	84.7	C-7	1038	10.38	883	8.83
	105.1	[b]C-15	194	1.94	165	1.65
G-7	9.4	C-5	1213	12.13	1032	10.32
	37.1	C-12	1717	17.17	1461	14.61
	62.1	C-14 Run 1	1675	16.75	1426	14.26
	↓	C-14 Run 2	1679	16.79	1429	14.29
		C-14 Run 3	1678	16.78	1428	14.28
		C-14 Run 4	1678	16.78	1428	14.28
	84.7	[b]C-15	930	9.30	792	7.92
	105.1	[b]C-15	202	2.02	172	1.72
J-3	9.4	C-13	1034	10.34	880	8.80
	62.1	C-12	1326	13.26	1128	11.28
	105.1	C-16	402	4.02	342	3.42
K-1	9.4	C-16	614	6.14	522	5.22
	37.1	C-11	999	9.99	850	8.50
	62.1	C-11	965	9.65	821	8.21
	84.7	C-1	709	7.09	603	6.03
	105.1	C-13	338	3.38	288	2.88
g-4	6.6	C-3	792	7.92	674	6.74
	37.1	C-1A	945	9.45	804	8.04
	62.1	C-1	954	9.54	812	8.12
	110.0	C-3	236	2.36	201	2.01
g-6	6.6	C-3	850	8.50	723	7.23
	37.1	C-5	1239	12.39	1055	10.55
	62.1	C-12	1162	11.62	989	9.89
	84.7	[b]C-15	543	5.43	462	4.62
	110.0	C-13	180	1.80	154	1.54

[a]$KG = 0.853\ R_C$.

[b]Suspected defective ionization chamber.

TABLE VI. - Concluded. RESULTS OF GRAPHITE IONIZATION CHAMBER MEASUREMENTS IN TWMR CRITICAL ASSEMBLY

Control tube or fuel element	Distance from core bottom plate to center of chamber, cm	Chamber number	Chamber reading with run normalization included, R_C		Absorbed gamma dose in graphite, KG[a]	
			rads	J/kg	rads	J/kg
g-8	6.6	C-2	858	8.58	731	7.31
	37.1	C-6	1411	14.11	1201	12.01
	62.1	C-2	1271	12.71	1082	10.82
	84.7	C-1A	913	9.13	777	7.77
	110.0	C-10	322	3.22	274	2.74
g-10	6.6	C-10	972	9.72	828	8.28
	37.1	C-7	1503	15.03	1279	12.79
	62.1	C-5	1442	14.42	1228	12.28
	84.7	C-13	1022	10.22	870	8.70
	109.7	C-6	353	3.53	301	3.01
g-12	6.6	C-9	986	9.86	839	8.39
	37.1	C-8	1811	18.11	1541	15.41
	62.1	C-7	1497	14.97	1274	12.74
	84.7	C-8	1259	12.59	1072	10.72
	110.0	C-9	347	3.47	296	2.96
h-8	6.6	C-16	1060	10.60	902	9.02
	37.1	C-10	1391	13.91	1184	11.84
	62.1	C-7	1342	13.42	1142	11.42
	84.7	C-8	1111	11.11	946	9.46
	110.0	C-9	301	3.01	256	2.56
j-4	6.6	C-9	725	7.25	617	6.17
	37.1	C-8	1248	12.48	1063	10.63
	62.1	C-2	1017	10.17	866	8.66
	84.7	[b]C-1A	219	2.19	187	1.87
	110.0	C-10	256	2.56	218	2.18
k-1	6.6	C-3	660	6.60	561	5.61
	37.1	C-6	1027	10.27	875	8.75
	62.1	C-2	914	9.14	778	7.78
	84.7	C-11	697	6.97	593	5.93
	110.0	C-1A	195	1.95	166	1.66

[a]KG = 0.853 R_C.

[b]Suspected defective ionization chamber.

COMPARISON OF CALCULATION AND MEASUREMENT OF ABSOLUTE GAMMA DOSE

The measured and calculated absolute gamma dose deposited in graphite are compared in figure 13 and in table III. For convenience in comparing the calculated and measured values, the solid lines shown in figure 13 enclose the band of probable error of the measured values. The calculated values are shown as bars indicating the one standard deviation confidence level. It is noted that the measured and calculated values agree within their mutual uncertainties in all but one case. Table III shows that the deviation between experiment and calculation is within 10 percent in 10 out of 16 locations compared.

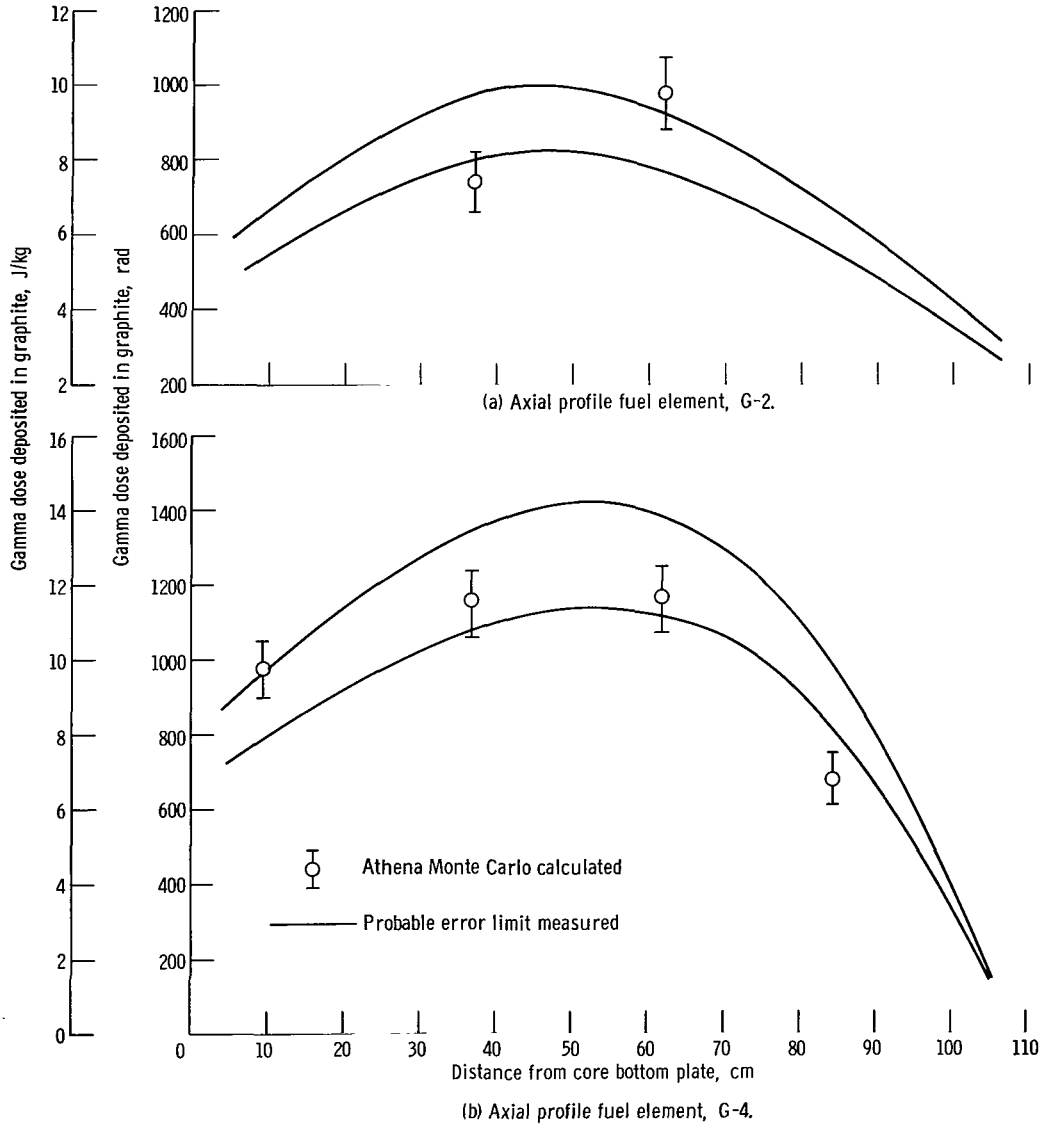

Figure 13. - Comparison of measured and calculated absolute gamma dose.

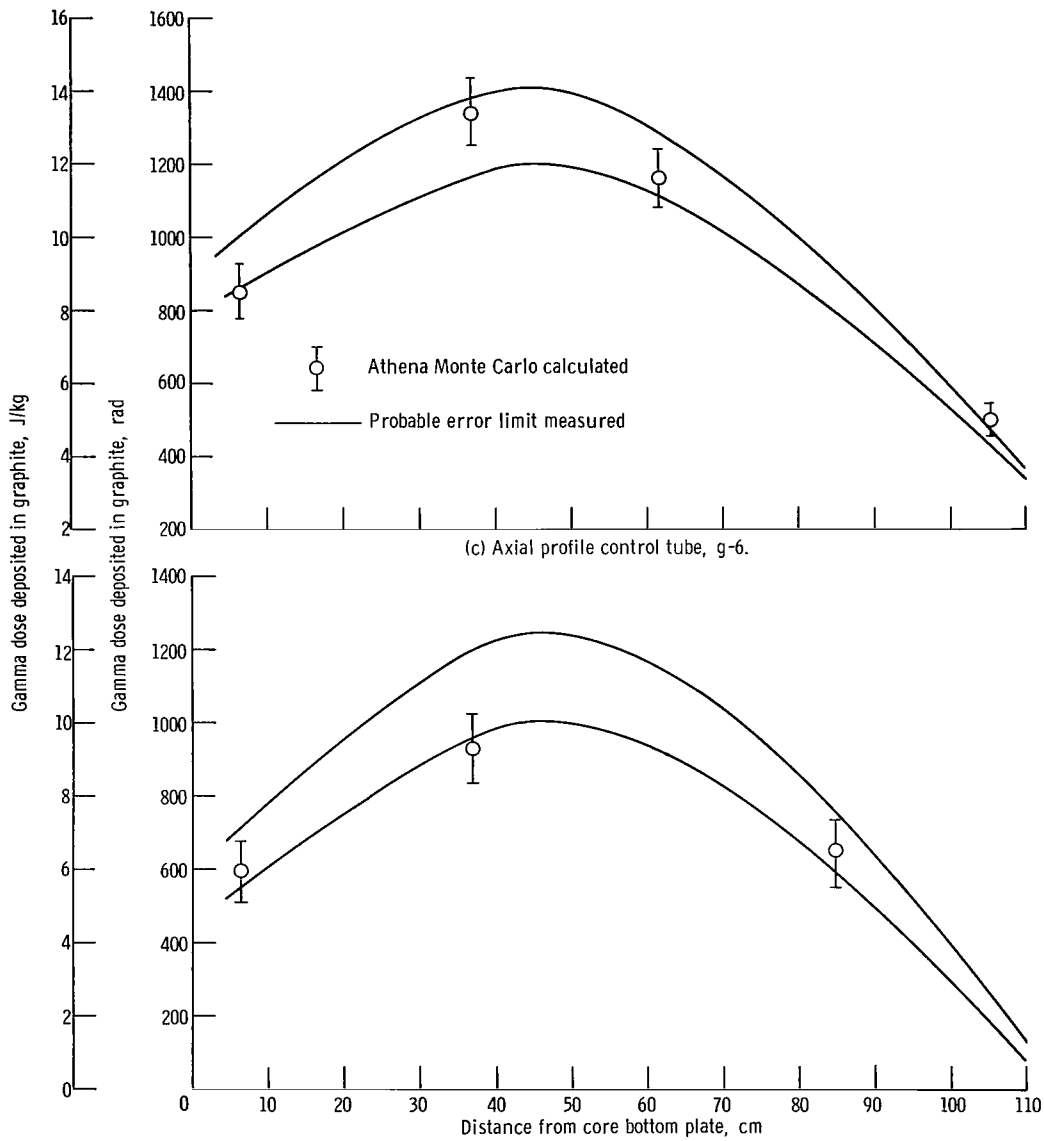

(c) Axial profile control tube, g-6.

(d) Axial profile control tube, g-10.

Figure 13. - Continued.

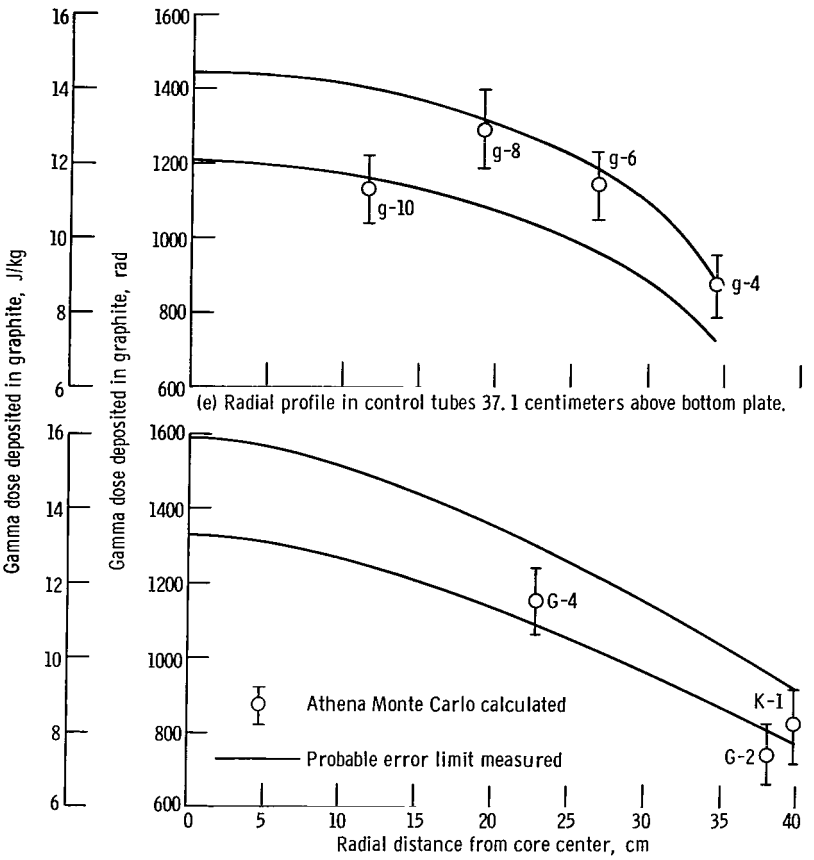

(e) Radial profile in control tubes 37.1 centimeters above bottom plate.

(f) Radial profile in fuel assemblies 37.1 centimeters above bottom plate.

Figure 13. - Concluded.

NEUTRON DOSE CALCULATIONS

The neutron dose in water is the result of elastic collisions of neutrons with the nuclei in the water. The recoiling nuclei deposit their kinetic energy as heat. The other processes by which neutron heating can occur are inelastic scattering, neutron capture, and charged particle reactions. Inelastic scattering is nonexistent in hydrogen but has a threshold above 6 MeV in oxygen. The inelastic scattering gamma rays were included in the gamma calculation but the small amount of kinetic energy deposited by the recoiling neutrons was ignored in the neutron dose calculations. The neutron capture gammas were included in the gamma calculations and the charged particle reactions were assumed to be negligible.

The method used to calculate neutron dose was outlined in connection with the calculation of ν in the section Correction for Neutron Sensitivity of Graphite Chambers. The total dose $D_{tot}(\vec{r})$ or energy deposited in 1 gram of material per unit time from fast neu-

trons at the position $\vec{r}$ is

$$D_{tot}(\vec{r}) = \int_{E_L}^{\infty} \mathcal{N}\sigma_s f E \varphi(E, \vec{r}) dE \tag{8}$$

where $\mathcal{N}$ is the atomic number density in atoms/gram, σ_s is the elastic scattering cross section of the atom, f is equal to $2M/(M+1)^2$ where M is the atomic mass, and $\varphi(E, \vec{r})$ is the neutron flux per unit energy centered about the energy E at the position of measurement $\vec{r}$ with the reactor operating at power.

In the calculation, the integral of equation (8) is replaced by a summation over a 30 group GAM II structure. The upper limit on the summation was taken at 14.9 MeV. The lower limit E_L was taken at 854 eV. The contribution to D_{tot} from neutrons outside this energy range is negligible.

$$D_{tot}^{H_2O}(\vec{r}) = A(\vec{r}) \sum_{j=1}^{j=30} \left(\mathcal{N}_H \sigma_{sj}^H f_H E_j \varphi_j \Delta U_j + \mathcal{N}_O \sigma_{sj}^O f_O E_j \varphi_j \Delta U_j \right) \tag{9}$$

The GAM II code is used to supply the group elastic scattering cross sections σ_{sj}.

The flux values φ_j are obtained from a radial three-region P_0S_4 transport unit cell calculation using the TDSN program (ref. 8). The central radial region in this calculation consisted of the homogenized uranium 235, uranium 238, aluminum, and tungsten in a fuel element. The next radial region contained the homogenized aluminum of the pressure tube and the two control tubes associated with the fuel element, and the cadmium within the control tubes. The outer radial region in the calculation contained the water in the moderator and in the control tubes associated with the fuel element. Thirty group spectrum averaged cross sections supplied by the GAM II code were used in each region. The TDSN calculated fluxes for each region are normalized to a source strength of 1 neutron per square centimeter of the cell volume. The multiplier $A(\vec{r})$ is used to renormalize the flux to that in the TWMR at the position $\vec{r}$ at power.

As previously stated, the shape of the GAM II computed neutron spectrum is dependent on the value of the input buckling. The input buckling used in the calculation of ν was used in this calculation.

The value calculated for the quantity within the summation sign in equation (9) was

$$4.399 \frac{\text{MeV}}{\text{g}(H_2O)} \frac{\text{cm}^3}{\text{fission neutron}} = 7.048 \times 10^{-10} \frac{\text{J cm}^3}{\text{kg}(H_2O) \text{ fission neutron}}$$

for the water region in the TDSN radial cell. Similarly, a value of

$$8.053\times10^{-10}\ \frac{\text{J cm}^3}{\text{kg}(H_2O)\ \text{fission neutron}}$$

was calculated for the fuel region.

The normalizing factor $A(\vec{r})$ was computed using the power distributions measured in the TWMR critical assembly. These power distributions were in good agreement with neutronic calculations. The power distributions in the TWMR critical assembly were separable; that is, the shape of the power distribution in the axial direction was independent of the radial position of the fuel element along which the axial measurements were made. The axial power shape used in the calculation is shown in figure 6. The radial power density at the midplane of the core normalized to unity at center fuel element is shown in table II.

The value $A(\vec{r})$ is the product of a radial factor $F_R(r)$ corresponding to the relative power density at the radius r at which the neutron dose is to be calculated, and an axial factor $F_A(z)$ corresponding to the power density at a distance z above the core bottom plate at which the calculation is made, and a constant factor corresponding to the power level of the critical assembly during the measurement.

The radial factor $F_R(r)$ when the ionization chamber is located within the fuel element is taken directly from table II. If the ionization chamber is located in a control tube, then the radial factor is the average value of the three adjacent fuel elements. The axial factor $F_A(z)$ is found using figure 6.

The constant factor is calculated using the absolutely measured total core power level of 84.2 watts and the 40 minute irradiation time and the 657 100 cubic centimeter TWMR core volume as follows:

$$84.2\ \text{W}\times 3.27\times10^{10}\ \frac{\text{fission}}{\text{W-sec}}\times 2.477\ \frac{\text{source neutrons}}{\text{fission}}\times 40\ \text{min}\times\frac{60\ \text{sec}}{\text{min}}$$

$$\times\frac{1}{657\ 100\ \text{cc}} = 2.491\times10^{10}\ \frac{\text{source neutrons}}{\text{cc}}$$

Thus, $A(\vec{r})$ is $2.49\times10^{10}\ F_R(r)\times F_A(z)$ and equation (9) becomes, in the water regions,

$$D_{tot}(\vec{r}) = 1.756\times10^{1}\ F_R(r) \times F_A(z)\ \frac{J}{kg(H_2O)}$$

$$= 1.756\times10^{3}\ F_R(r) \times F_A(z)\ \text{(rads)} \qquad (10)$$

Similarly, in the fuel regions

$$D_{tot}(\vec{r}) = 2.006\times10^{3}\ F_R(r) \times F_A(z)\ \text{rads};\ 2.006\times10^{1}\ F_R(r) \times F_A(z)\ J/kg(H_2O)$$

RESULTS AND ERROR ANALYSIS OF NEUTRON DOSE CALCULATIONS

The calculated neutron dose is given in table VII. The errors in these calculations result from the uncertainty in the GAM II computed neutron spectrum caused by sensitivity of the spectrum to the buckling and the uncertainty in the power distribution used in the calculations.

If the input buckling to the GAM II spectrum calculation is decreased by 30 percent to the overall epithermal buckling value used for neutronic calculations for the core, the value computed for the sum in equation (9) is increased by 7 percent. The uncertainty in the power distributions is about ±5 percent. The total error associated with the calculation is therefore ±6 percent assuming that the error connected with the buckling input to GAM II is one-sided and, therefore, contributes only ±3.5 percent to the total error.

TOTAL RADIATION DOSE MEASUREMENTS

The total radiation dose measurements were made using the gamma sensitive graphite chambers previously described and the neutron sensitive polyethylene chambers to be described. Both the graphite and the polyethylene chambers were absolutely calibrated in the bremsstrahlung gamma beam of the Electron Linear Accelerator (Linac) at General Atomic and gamma response coefficients (chamber dose reading per unit rad (J/kg) gamma dose in water) obtained. This calibration (for the graphite chambers) has already been described.

The graphite and polyethylene chambers were then irradiated in the mixed neutron and gamma spectrum in the TRIGA reactor at General Atomic. The total radiation deposition to water was absolutely measured at the test location with the TRIGA reactor using a water-filled calorimeter.

TABLE VII. - RESULTS OF POLYETHYLENE IONIZATION CHAMBER CALCULATIONS AND MEASUREMENTS IN TWMR CRITICAL ASSEMBLY

Control tube or fuel element	Distance from core bottom plate to center of chamber, cm	Calculated neutron dose in water		Measured neutron dose in water		Percent difference
		rads	J/kg	rads	J/kg	
G-2	9.4	1760	17.6	----	----	---
	37.1	2260	22.6	----	----	---
	62.1	2160	21.6	----	----	---
	67.0	2060	20.6	2180	21.8	-5
	105.1	739	7.39	----	----	---
G-4	9.5	2120	21.2	----	----	---
	[a]32.4	2650	26.5	2230	22.3	+19
	37.1	2710	27.1	----	----	---
	62.1	2590	25.9	----	----	---
	67.0	2470	24.7	3660	36.6	-32
	84.7	1840	18.4	----	----	---
	105.1	888	8.88	----	----	---
g-4	6.6	1630	16.3	----	----	---
	11.4	1530	15.3	1560	15.6	-2
	32.4	1910	19.1	2390	23.9	-20
	37.1	1970	19.7	----	----	---
	62.1	1880	18.8	----	----	---
	67.0	1790	17.9	2280	22.8	-22
	80.0	1600	16.0	2000	20.0	-20
	105.3	630	63	810	8.10	-22
	110.0	444	4.44	----	----	---
g-8	6.6	2060	20.6	----	----	---
	11.4	1930	19.3	2350	23.50	-18
	32.4	2420	24.2	3200	32.0	-24
	37.1	2490	24.9	----	----	---
	62.1	2380	23.8	----	----	---
	80.0	1880	18.8	2520	25.2	-25
	84.7	1690	16.9	----	----	---
	105.3	797	7.97	1130	11.3	-29
	110.0	562	5.62	----	----	---
g-12	6.6	2290	22.9	----	----	---
	[a]11.4	2160	21.6	2060	20.6	+5
	[a]32.4	2700	27.0	3410	34.1	-21
	37.1	2760	27.6	----	----	---
	62.1	2630	26.3	----	----	---
	[a]67.0	2520	25.2	1620	16.2	+55
	[a]80.0	2080	20.8	2970	29.7	-30
	84.7	1870	18.7	----	----	---
	[a]105.3	840	84.0	970	9.7	-9
	110.0	630	63.0	----	----	---

[a]Suspected defective ionization chamber.

TABLE VII. - Concluded. RESULTS OF POLYETHYLENE IONIZATION CHAMBER CALCULATIONS AND MEASUREMENTS IN TWMR CRITICAL ASSEMBLY

Control tube or fuel element	Distance from core bottom plate to center of chamber, cm	Calculated neutron dose in water		Measured neutron dose in water		Percent difference
		rads	J/kg	rads	J/kg	
h-8	6.6	2090	20.9	----	----	---
	[a]11.4	1970	19.7	1110	11.1	+78
	32.4	2460	24.6	2960	29.6	-17
	37.1	2530	25.3	----	----	---
	62.1	2410	24.1	----	----	---
	[a]67.0	2310	23.1	1500	15.0	+53
	80.0	1900	19.0	2590	25.9	-26
	84.7	1710	17.1	----	----	---
	105.3	810	8.1	860	8.6	+6
	110.0	570	5.7	----	----	---
j-4	6.6	1710	17.1	----	----	---
	11.4	1620	16.2	1550	15.5	+5
	32.4	2020	20.2	2490	24.9	-19
	37.1	2070	20.7	----	----	---
	62.1	1980	19.8	----	----	---
	67.0	1880	18.8	2630	26.3	-28
	80.0	1570	15.7	2000	20.0	-22
	84.7	1410	14.1	----	----	---
	105.3	663	6.63	1050	10.5	-37
	110.0	468	4.68	----	----	---
k-1	6.6	1670	16.7	----	----	---
	11.4	1580	15.8	1570	15.7	0
	32.4	1970	19.7	2270	22.7	-13
	37.1	2020	20.2	----	----	---
	62.1	1930	19.3	----	----	---
	67.0	1840	18.4	2130	21.3	-14
	84.7	1380	13.8	----	----	---
	105.3	647	6.47	724	7.24	-11
	110.0	457	4.57	----	----	---

[a]Suspected defective ionization chamber.

The Linac and the TRIGA measurements were then combined with equation (1) to determine a gamma response coefficient ϵ and a neutron response coefficient δ for the polyethylene chamber analogous to the gamma response coefficient K and the neutron coefficient ν for the graphite chambers given in equation (1). The gamma or neutron response coefficients are defined as chamber dose reading per unit gamma or neutron rad (J/kg) dose in water.

Having thus obtained neutron and gamma response coefficients for the graphite and polyethylene chambers, it was possible to solve independently for the neutron dose to water at the calibration location in the TRIGA reactor, and at each measurement location in the TWMR reactor. The average ratio of gamma dose to total dose $\bar{S}$ for each reactor can thus be determined.

Description of Polyethylene Ionization Chambers

Nine polyethylene wall, ethylene-filled chambers were used. These chambers were sensitive to both gamma rays and fast neutrons. The chambers were 1.85 inches (4.67 cm) long and had an ionizable volume of 0.040 cubic centimeter. The outer diameter of the chambers was 0.490 inch (1.245 cm) for the same reasons as the graphite wall dosimeters. Figure 14 shows a schematic of the polyethylene chamber. The resulting

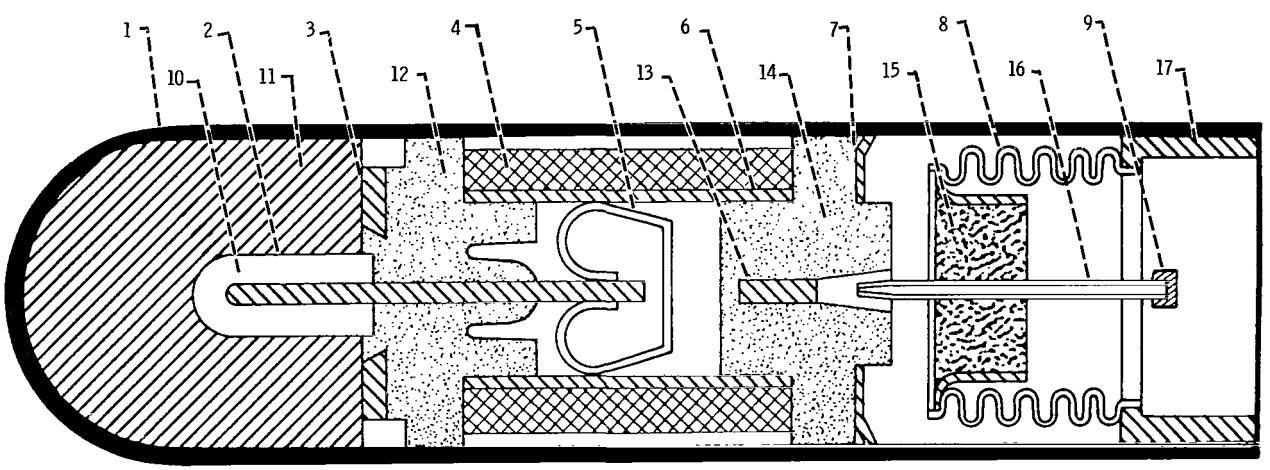

1, Aluminum shell (1.850 in. long - 0.490 in. diam - 0.015 in. wall)
2, Aluminum electrode (0.025 in. diam)
3, Bakelite shield
4, Condenser (3000 pF)
5, Electrode clip
6, Aluminum condenser core
7, Retainer ring
8, Bellows assembly
9, End cap
10, Ionizable volume 0.040 cm^3 (ethyelene gas)
11, Polyethelyene chamber (0.165 in. wall)
12, Electrode insulator
13, Electrode contact bar
14, Condenser insulator
15, Glass seal
16, Contact pin
17, End sleeve

Figure 14. - 5000 rad polyethylene ionization chamber details.

polyethylene wall thickness of 0.385 gram per square centimeter exceeded the range of 1.0 MeV and thus provided an equilibrium thickness for 1.25-MeV gamma rays.

Since the polyethylene chambers were placed mainly in poison tubes, they were, in most measurements, surrounded by water which increased the effective wall thickness. The absorbed dose in water and polyethylene varies by only 3 percent in the Compton region and therefore the maximum error caused by the walls not being infinite was about 3 percent.

Calibration of Polyethylene Chambers

First, the gamma response of the polyethylene chambers was absolutely determined using the bremsstrahlung beam of the Linac. This calibration was identical with that for the graphite chambers discussed above. The results of this calibration is given in table V and figure 15.

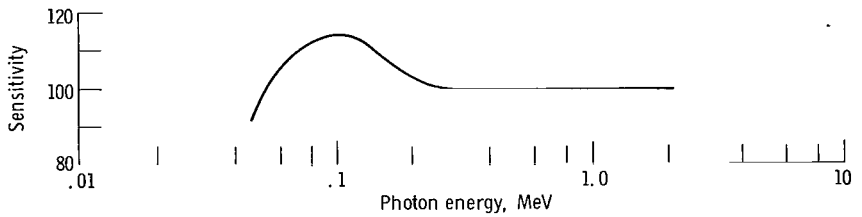

Figure 15. - Typical polyethylene ionization chamber response curve.

Second, the response of the polyethylene chambers to the mixed gamma plus neutron radiation spectrum within the General Atomic TRIGA reactor was absolutely measured by comparison against a specially designed water-filled calorimeter. Ideally, this calibration should have been made in the mixed radiation spectrum of the TWMR core since the calibration would then be directly applicable to the data measured there. However, the allowable flux levels in the TWMR were insufficient to cause an appreciable rise in the water bath temperature of calorimeter, and so the calibration was made in the high-power density TRIGA core. It was therefore necessary to determine the ratio of the gamma to total gamma plus neutron dose $\overline{S}$ for each of the cores and apply suitable corrections to the data.

Houghton, Jupiter, and Trimble (ref. 2) designed the calorimeter and made the dose measurements. The outer jacket of the calorimeter was held to a maximum diameter of 1.250 inches (3.17 cm) to allow it to fit into a tube in the TRIGA core. Since the size was restricted, they used an adiabatic jacket to reduce heat transfer between the water ab-

sorbing mass and its environment. This adiabatic jacket was placed halfway between the outer jacket and the water mass and was made of aluminum and epoxy with a heating coil potted into the epoxy; adjustment of the power dissipated in the coil almost completely eliminated heat transfer between the water mass and its environment. They further reduced heat transfer by using fine (0.006 in. (0.0152 cm) diameter) copper connection wires to lead into the water mass and keeping all heat paths between the water mass and the adiabatic jacket long and of small cross sectional area. All interior surfaces were painted white and the area around the jacket was evacuated. Since the neutron and gamma energy would be absorbed by the vessel walls as well as by the water, they designed the vessel to have a small mass compared with the water mass. Sheet polyvinyl chloride (PVC) was thermoformed into a two-piece bottle with approximately 0.004-inch (0.010 cm) thick walls. A thin (~0.002 in. (0.0051 cm)) coating of epoxy was painted on the outside of the vessel to eliminate vapor pumping since the PVC is not impervious to water vapor. Details of the calorimeter are shown in figure 16.

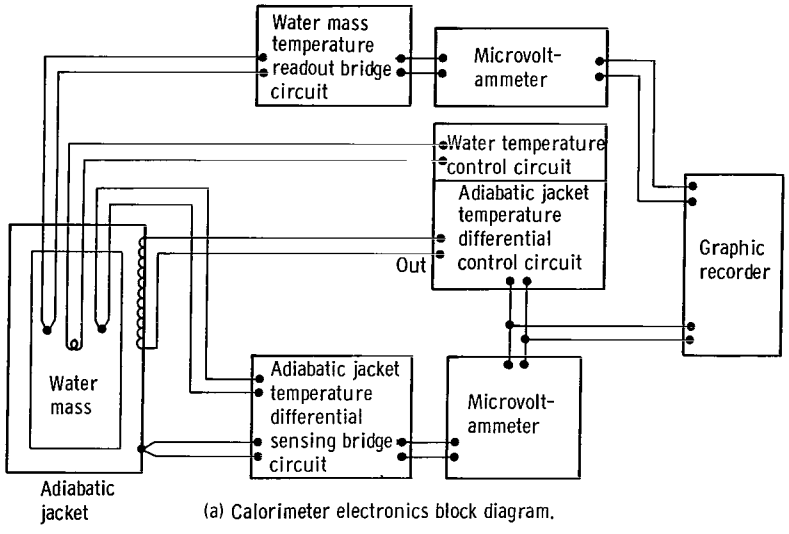

(a) Calorimeter electronics block diagram.

Figure 16. - Calorimeter details.

Fine control of the temperature difference between the water mass and the adiabatic jacket and the ability to accurately sense small incremental temperature changes in the water mass dictated the use of thermistors as temperature sensing elements. The thermistors had a nominal resistance of 25° C of 50 000 ohms, a spherical diameter of 0.043 inch (0.109 cm) and a temperature coefficient of resistance of 4.5 percent per Centigrade degree. A pair of these thermistors, matched to within 0.2 percent of each other, was imbedded, one in the adiabatic jacket and one in the water mass: it forms two legs of a bridge circuit as shown in figure 16(c) and is used to control the temperature of the

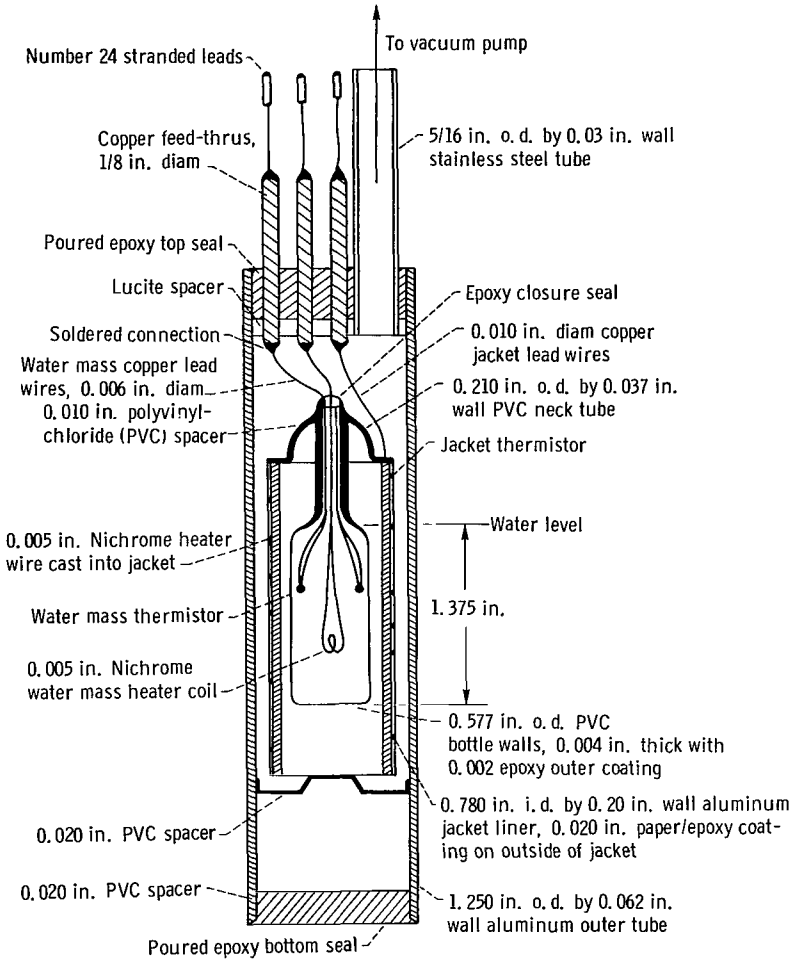

(b) Cross section of calorimeter.

Figure 16(b). - Continued.

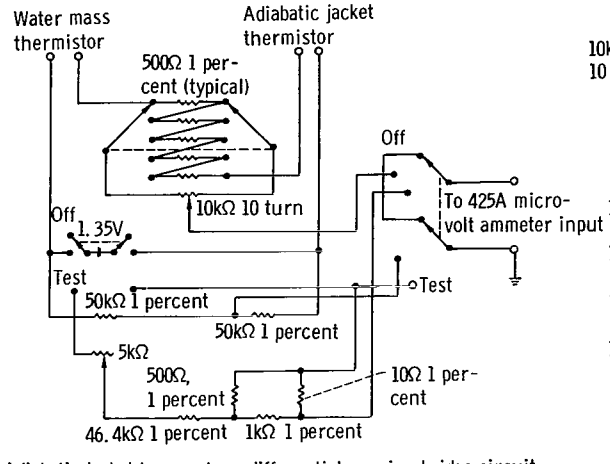

Adiabatic jacket temperature differential sensing bridge circuit

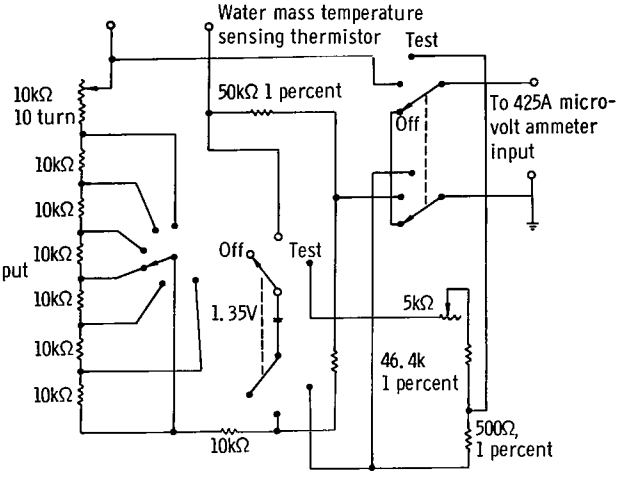

Water mass temperature sensing bridge circuit

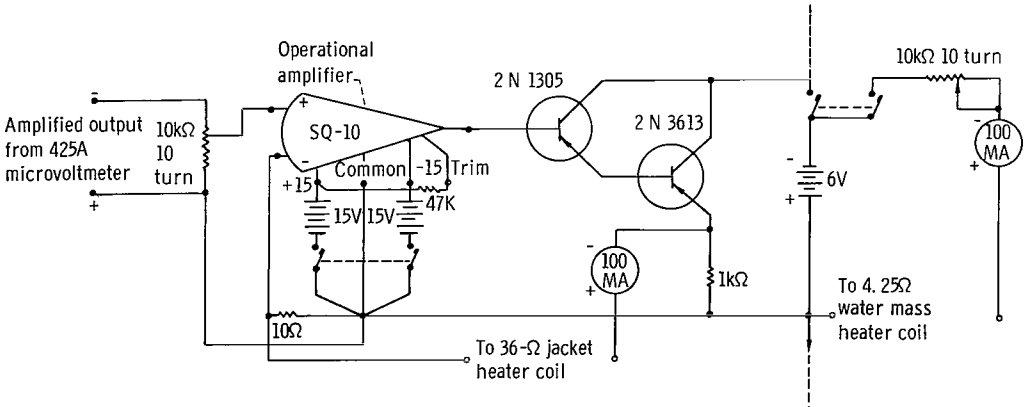

Adiabatic jacket temperature differential control circuit

Water mass temperature control circuit

Figure 16(c). - Concluded.

adiabatic jacket with respect to the water mass to eliminate heat transfer. An additional thermistor in the water mass forms one leg of the other bridge circuit of figure 16. This was carefully calibrated to allow accurate monitoring of the rate of temperature rise in the water mass. Houghton and his coworkers (ref. 2) calibrated the thermistor as follows: The entire water mass assembly was placed in a large volume of water contained by a vacuum-jacketed glass-walled flask. A copper-constantan thermocouple was located on the surface of the calorimeter water mass and, using an ice bath cold junction, connected to a precision potentiometer which allowed accurate determination of the temperature of the water bath. A battery-driven resistance heater was used to raise slowly the temperature of the water bath and the calorimeter water mass assembly suspended within it. The output of the bridge circuit as a function of temperature change was monitored by a microvoltmeter and a strip chart recorder, and was found to be 14.85 millivolts per ^{o}C which agreed very well with calculations based on the manufacturer's rated temperature coefficient of resistance. This constant was used in the analysis of subsequent measurements. A 4.25-ohm heater coil was included in the water absorbing mass to control the temperature and provide a check on the operation of the system.

Once the jacket controls were correctly adjusted, they (ref. 2) tested the calorimeter by applying power to the water mass coil and observing the rate of temperature rise of the water mass on the strip-chart recorder. The slope of the temperature rise curve (in mV/min) gives the heating rate since the thermistor constant is known to be 14.85 millivolts per ^{o}C.

When the calorimeter was operated in the TRIGA reactor, a temperature rise rate of 0.0829^{o} C per minute was observed at a steady-state reactor power level of 10 kilowatts; this rate was obtained from the recorder trace which showed a voltage change rate (due to the change in resistance in the calibrated thermistor in the water mass) of 1.23 millivolts per minute. Since 0.0829^{o} C per minute corresponds to 0.0829 gram-calorie per gram per minute for pure water at 13^{o} C (the temperature of the reactor water during the calibration runs) the heat input rate to the calorimeter water mass is given by

$$0.0829 \frac{\text{g-cal}}{\text{g-min}} \; 4.19\times10^{7} \frac{\text{ergs}}{\text{g-cal}} = 3.47\times10^{6} \frac{\text{ergs}}{\text{g-min}}$$

and the dose rate in water at 10 kilowatts is

$$\frac{3.47\times10^{6} \dfrac{\text{ergs}}{\text{g-min}}}{10^{2} \dfrac{\text{ergs}}{\text{g-rad}}} = 3.47\times10^{4} \frac{\text{rads}}{\text{min}} \; (3.47\times10^{2} \text{ J kg}^{-1} \text{ min}^{-1})$$

The reactor power level during the irradiation of the dosimeters was 1.8 kilowatts;

therefore the dose rate in water corresponding to the readings of the dosimeters is 6250 rads per minute (62.5 J kg^{-1} min^{-1}).

As a check on the calorimeter operation, the reactor was operated at 20 kilowatts with a heating rate of 0.167° C per minute being obtained in the calorimeter water mass. Doubling the power doubles the heating rate which indicates that the relative power rates of the reactor are well known and that the calorimeter is able to accurately follow the reactor power level changes.

The results of the absolute calibration of the polyethylene chambers against a water calorimeter are shown in table VIII. Also shown is the calibrated rad reading of several graphite chambers which were placed in the same reactor core position as the polyethylene chambers.

TABLE VIII. - CALIBRATION OF ION CHAMBERS IN TRIGA REACTOR

(a) Polyethylene ionization chamber; TRIGA calorimeter dose 6250 rads (62.5 J/kg)

Ionization chamber number	Chamber reading, percent of full scale			Full-scale average corrected chamber reading	
	Uncorrected reading	Position correction	Corrected reading	rads	J/kg
P-1	49.5	0.982	48.6	12 860	128.6
P-2	41.1	1.02	41.9	14 920	149.2
P-3	43.4	1.02	44.3	14 090	140.9
P-4	45.0	.982	44.1	14 190	141.9
P-5	43.1	1.02	43.9	14 220	142.2
P-6	55.4	.982	54.4	11 400	114.0
P-6	56.3	.982	55.3	11 310	113.1
P-7	50.4	1.02	51.4	12 150	121.5
P-8	51.5	.982	50.6	12 360	123.6
P-9	43.5	.982	42.7	14 620	146.2
P-9	41.3	1.02	42.2	14 810	148.1
P-9	42.4	1.02	43.3	14 420	144.2

(b) Graphite ionization chamber

Ionization chamber number	Chamber reading, percent of full scale			Graphite chamber reading in TRIGA reactor, R''_C	
	Uncorrected reading	Position correction	Corrected reading	rads	J/kg
C-2	60.8	1.02	62.0	2 246	22.46
C-5	57.4	1.02	58.6	2 309	23.09
C-9	53.3	1.02	54.3	2 193	21.93
C-14	56.5	.982	55.5	2 157	21.55
Average				2 226	22.26

Positioning and Irradiation of Polyethylene Chambers in TWMR Critical Assembly

The positioning and irradiation of the polyethylene chambers in the TWMR critical assembly have been described in connection with the graphite chambers in previous sections Positioning of Graphite Chambers in TWMR Critical Assembly and Irradiation of Chambers in TWMR.

Analysis of Total Dose Data

The gamma sensitive graphite chambers and the polyethylene neutron sensitive chambers responded to some extent to both neutrons and photons. Therefore, the total dose calibration of the chambers against the water-filled calorimeter in the mixed neutron and gamma radiation spectrum of the TRIGA reactor could not be directly applied to the total dose measurements in the TWMR, which had a different mixed radiation field. The data measured in the Linac and the TRIGA reactor was therefore used to determine individual response coefficients for neutrons and for gammas for the graphite chambers and the polyethylene chambers. These response coefficients were then applied to the TRIGA and the TWMR critical assembly dose measurements to obtain the gamma dose and the neutron dose separately at each position measured. In addition average spectral indices, that is, the average ratio of the gamma dose in water to the total mixed gamma plus neutron radiation dose in water, were determined for the TRIGA reactor and for the TWMR critical assembly and were found to differ by 20 percent.

Determination of chamber response coefficients. - The chamber response coefficients ϵ, δ, K, ν are defined as follows:

For the polyethylene chamber,

$$R_p = \epsilon G + \delta N \tag{11}$$

For the graphite chamber,

$$R_C = KG + \nu N \tag{12}$$

where R_p is the reading of the polyethylene chamber for mixed radiation dose of G rads (J/kg) gamma dose plus N rads (J/kg) neutron dose measured in water, ϵ is the dose reading of the polyethylene chamber per rad (J/kg) of gamma dose in water, G is the rad (J/kg) gamma dose at the position of measurement in water, δ is the dose reading of the

polyethylene chamber per rad (J/kg) neutron dose in water, N is the rads (J/kg) neutron dose measured in water, R_C is the reading of the graphite chamber for the mixed radiation dose of G rads (J/kg) gamma dose plus N rads (J/kg) neutron dose measured in water, K is the response of the graphite chamber per rad (J/kg) gamma dose in water, and ν is the response of the graphite chamber per rad (J/kg) neutron dose in water.

In the Linac calibration both the polyethylene chambers and the graphite chambers were irradiated to a graphite dose level of B rads (0.01 B J/kg) as measured by the standard calibration chamber in a 7.0-MeV bremsstrahlung beam. This beam contained no neutrons because the maximum beam photon energy was below the threshold for γ,n reactions.

Therefore, the readings on the chambers using equations (11) and (12) are

$$R'_p = \epsilon \left[\left(\frac{D_{H_2O}{}^{\gamma}}{D_C{}^{\gamma}} \right) B \right] \tag{13}$$

$$R'_C = K \left[\left(\frac{D_{H_2O}{}^{\gamma}}{D_C{}^{\gamma}} \right) B \right] \tag{14}$$

where R'_p and R'_C are the scale readings of polyethylene and graphite chambers when irradiated to a dose of B gamma rads (0.01 B J/kg) in graphite, and $\left(D_{H_2O}{}^{\gamma}/D_C{}^{\gamma}\right)$ is the ratio of gamma dose deposited in water to gamma dose deposited in graphite. This conversion factor is required since the response coefficients ϵ and K are defined as the response per rad (J/kg) gamma dose in water. The response coefficients ϵ and K are therefore:

$$\epsilon = \frac{R'_p}{\left(\frac{D_{H_2O}{}^{\gamma}}{D_C{}^{\gamma}} \right) B} \tag{15}$$

and

$$K = \frac{R'_C}{\left(\frac{D_{H_2O}{}^{\gamma}}{D_C{}^{\gamma}} \right) B} \tag{16}$$

The average value of the polyethylene chamber response coefficient ϵ is computed to be $\bar{\epsilon} = 1.26$ in table V using $\left(D_C^{\gamma}/D_{H_2O}^{\gamma}\right) = 0.9009$. The full scale rad (J/kg) values for the polyethylene chambers shown in table V were determined in the calibration of these chambers against the water-filled calorimeter in TRIGA reactor which is discussed later.

The graphite chambers were absolutely calibrated by this irradiation and the full scale reading of each chamber determined by dividing the standard calibrating chamber measured dose B by the decimal fraction of full scale read on the chamber. Thus R'_C was set equal to B in equation (14) and therefore the response coefficient $K = D_C^{\gamma}/D_{H_2O}^{\gamma} = 0.9009$.

In the calibration in the TRIGA reactor, the reading of each chamber, R''_p and R''_C was compared against the total radiation deposition C, in rads (J/kg) measured by the temperature rise of the water mass in the calorimeter. Thus,

$$R''_p = \bar{\epsilon}G'' + \delta N'' \tag{17}$$

$$R''_C = KG'' + \nu N'' \tag{18}$$

and

$$C = G'' + N'' \tag{19}$$

where G'' is the rad (J/kg) gamma dose deposited in the water at the position of measurement in the TRIGA reactor and N'' is the rad (J/kg) neutron dose deposited in the water at the position of measurement in the TRIGA reactor.

The polyethylene chambers were absolutely calibrated by this irradiation and the full scale reading of each chamber determined by dividing the calorimeter measured dose C by the decimal fraction of the full scale reading on the chamber. Thus, R''_p was set equal to C for this irradiation. The results of this calibration are given in table VIII.

There are, then, three unknowns in equations (17) to (19), namely, δ, G'', and N''. The response of the graphite chamber per rad (J/kg) gamma dose in water ν was calculated as the ratio of the neutron dose per gram of carbon dioxide to neutron dose per gram of water in the section Correction for Neutron Sensitivity of Graphite Chambers.

By simultaneous solution, the values for these unknowns for the calibration are obtained as

$$G'' = \frac{R''_C - \nu C}{K - \nu} \tag{20}$$

$$N'' = \frac{R_C'' - KC}{\nu - K} \tag{21}$$

and

$$\bar{\delta} = \frac{R_p'' - \bar{\epsilon}G''}{N''} = \frac{C(\nu - K - \bar{\epsilon}\nu) + \bar{\epsilon}R_C''}{R_C'' - KC} \tag{22}$$

The average value calculated for δ using the values in table V was $\bar{\delta} = 0.861$. Thus, the general equations with the response coefficients inserted are

$$R_p = 1.26G + 0.861N \tag{23}$$

$$R_C = 0.901G + 0.0634N \tag{24}$$

These equations were then used to determine the absolute values of G and N from the measurements in the TRIGA reactor and in the TWMR critical assembly.

Methods for obtaining gamma and total dose in TWMR critical assembly. - The method for obtaining the absolute gamma dose was explained in the section Correction for Neutron Sensitivity of Graphite Chambers to require the solution of equation (1) for KG and the substitution of the spectrum index $S \equiv G/(G + N)$ in the equation to obtain

$$KG = R_C\left[\frac{1}{1 + \frac{\nu}{K}\left(\frac{1}{\bar{S}} - 1\right)}\right] \tag{2}$$

The unknown factor in this equation is the average value of the spectral index $\bar{S}$ for the TWMR critical assembly. This was obtained by solving equations (23) and (24) for N and G and then computing the value of $S = G/(G + N)$ at 23 polyethylene chamber core locations and then computing the core average. The equations for G, N, and S as obtained from equations (23) and (24) are

$$N = 1.29R_p - 1.81R_C \tag{25}$$

$$G = 1.24R_C - 0.0911R_p \tag{26}$$

$$S = \frac{G}{N + G} = \frac{1.24R_C - 0.0911R_p}{1.20R_p - 0.570R_C} \tag{27}$$

TABLE IX. - DATA MEASURED WITH POLYETHYLENE CHAMBERS IN TWMR AND CALCULATION OF AVERAGE SPECTRUM INDEX $\bar{S}$

Poison tube or fuel element	Distance from core bottom plate to center of chamber, cm	Chamber reading with run normalization included, R_p		Interpolated values of R_C		Spectrum index, $G/(G + N)$
		rads	J/kg	rads	J/kg	
G-2	67.0	3000	30.0	935	9.3	0.289
G-4	[a]32.4	----	----	----	----	-----
	67.0	4540	45.4	1210	12.1	0.228
g-4	11.4	2345	23.4	810	8.1	0.336
	32.4	3150	31.5	930	9.3	.267
	67.0	3070	30.7	930	9.3	.278
	80.0	2670	26.7	795	7.9	.270
	105.3	1105	11.1	340	3.4	.284
g-8	11.4	3223	32.2	1000	10.0	0.268
	32.4	4380	43.8	1355	13.5	.286
	80.0	3360	33.6	1000	10.0	.270
	105.3	1490	14.9	445	4.5	.271
g-12	[a]11.4	3370	33.7	1260	12.6	-----
	[a]32.4	5030	50.3	1765	17.7	-----
	[a]67.0	----	----	----	----	-----
	[a]80.0	4040	40.4	1230	12.3	-----
	[a]105.3	1470	14.7	510	5.1	-----
h-8	[a]11.4	----	----	----	----	-----
	32.4	4210	42.1	1360	13.6	0.304
	[a]67.0	----	----	----	----	-----
	80.0	3660	36.6	1180	11.8	.304
	105.3	1360	13.6	480	4.8	.347
j-4	11.4	2405	24.1	860	8.6	0.354
	32.4	3630	36.3	1210	12.1	.319
	67.0	3510	35.1	1050	10.5	.272
	80.0	2730	27.3	840	8.4	.283
	105.3	1305	13.1	350	3.5	.231
k-1	11.4	2285	22.9	760	7.6	0.318
	32.4	3180	31.8	1010	10.1	.297
	67.0	2890	28.9	880	8.8	.279
	105.3	1034	10.3	345	3.5	.320
g-16	23.5	4540	45.4	----	----	-----
	23.5	4620	46.2	----	----	-----
	23.5	4530	45.3	----	----	-----
	23.5	4620	46.2	----	----	-----
Average						0.290±0.026

[a]Suspected defective ionization chamber.

Since the computations of S are made at the core locations of the polyethylene chambers the values of R_p can be directly obtained from table IX. The values of R_C were obtained by interpolation of the plotted measurements of R_C given in table VI.

Table IX shows the computation of S at the 23 core locations and computation of the average value $\bar{S}$. The average value of S in the TWMR is $\bar{S} = 0.290$, which is then substituted into equation (2) and the rad (J/kg) gamma dose in graphite KG computed using equation (6)

$$KG = 0.853R_C$$

COMPARISON OF CALCULATION AND MEASUREMENT OF ABSOLUTE NEUTRON DOSE

The neutron dose was computed from the experimental data given in table IX using equation (25). The measured results are compared with the calculated results in table VII.

The calculated values of the neutron dose are consistently low in comparison with the measurements which are considered reliable with a deviation from the measurement between -11 and -28 percent in 15 out of the 23 locations investigated.

The error in the neutron dose measurements was estimated on the basis of the uncertainty in the polyethylene and graphite dosimeter measurements and on the uncertainty of the absolute power measurement. Using equation (25), the uncertainties in the chamber readings are related to the uncertainty in the neutron dose ΔN by

$$\Delta N = \sqrt{1.66\left(\Delta R_p\right)^2 + 3.27\left(\Delta R_C\right)^2} \tag{28}$$

where the constants are determined using typical values of N = 3200, R_p = 4380, and R_C = 1355. The uncertainty in R_p consists of a ±2 percent uncertainty in the reading of the polyethylene dosimeter, an ±8 percent uncertainty in the absolute calibration of the calorimeter, and a ±3 percent uncertainty in the time at which the TWMR critical assembly was at power. Combination of these uncertainties results in a ±9 percent error in the value of R_p.

The comparable error in R_C is ±6 percent and was discussed in the section Error Analysis of Gamma Dose Measurements.

The error in N obtained from equation (28) is ±17 percent. If the ±7 percent uncertainty in the absolute power level is incorporated, the total error in the measured neutron dose is ±18 percent. Figure 17 shows typical comparisons between the calculated and measured neutron dose distribution.

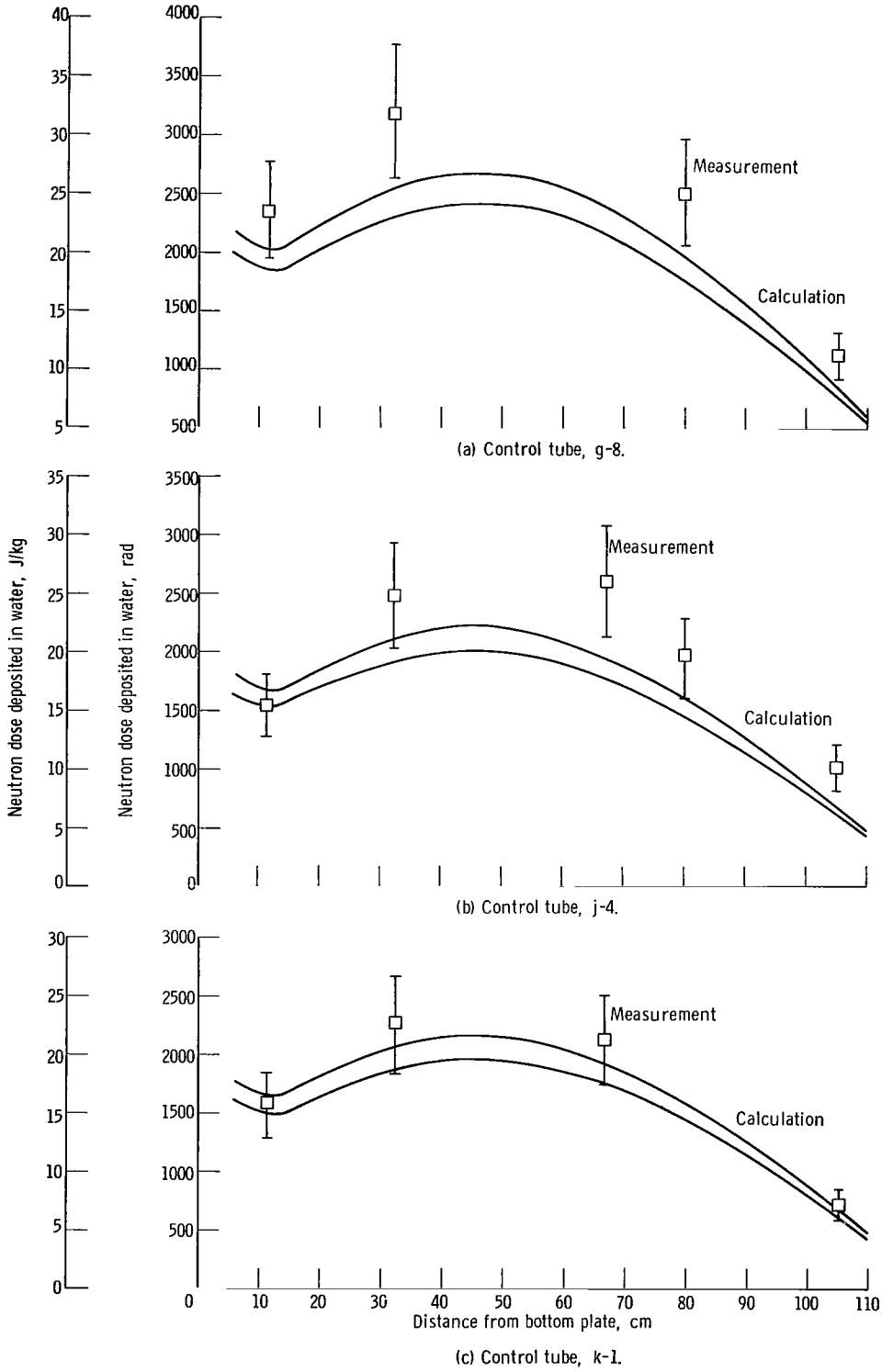

Figure 17. - Comparison of measured and calculated neutron dose.

COMPARISON OF CALCULATION AND MEASUREMENT OF TOTAL DOSE

Because of limitations on core storage, ATHENA calculations were made only at the positions of the graphite chambers and so a direct total dose calculated at the positions of the polyethylene chambers was not obtained. However, since good agreement was found between the measured and calculated gamma dose as discussed in the preceding section and since the gamma dose contributes only about 30 percent of the total dose, only a small error would result if the measured gamma dose were used in place of the calculated dose. Thus, the calculated total radiation dose was computed as the sum of measured gamma dose and the calculated neutron dose. The calculated total dose computed in this way is compared with the measured total dose in table X. The calculated values of the total dose are consistently smaller than the measured values. The calculations underestimated the measurement by less than 17 percent in 17 out of the 23 locations investigated. This difference is caused by the underestimation of the neutron dose discussed earlier.

MEASUREMENT OF ABSOLUTE POWER LEVEL

The measurement of the absolute power level was based on the measured critical assembly relative power distributions and a calculated conversion factor relating the subcadmium activity of gold foils to the fission power at the center of the critical assembly. The radial power distributions were measured in detail by counting the fuel element fission product activity in one symmetrical one twelfth sector at the midplane of the critical assembly (see fig. 10). The relative axial power distributions were measured at 24 heights at three different fuel element locations also by counting the fission product activity.

The axial and radial power distributions measured were found to be independent so that the local power density to average core power density at the point (r, z) was simply the product of the relative radial power density at the radius r times the relative axial power density at the height z divided by product of the volume integrated relative radial and axial distributions. Table II gives the measured relative radial power density at the midplane of the TWMR critical assembly and figure 6 shows the measured axial power distribution in the center fuel element.

The conversion factor relating the subcadmium activity to the power in the center of the assembly was evaluated using GAMBLE (ref. 9) computed fluxes and transport-theory-determined disadvantage factors appropriate to the position of the foils adjacent to center fuel element at the midplane of the core.

The absolute core power for a reactor run was then determined by dividing the measured absolute saturated subcadmium activity by the product of the calculated conversion factor and the measured local to average core power at the center of the assembly.

TABLE X. - COMPARISON OF CALCULATED AND MEASURED TOTAL DOSE IN TWMR CRITICAL ASSEMBLY

Control tube or fuel element	Distance from core bottom plate to center of chamber, cm	Total heating dose in water				Percent deviation
		Calculated		Measured		
		rads	J/kg	rads	J/kg	
G-2	67.0	2950	29.5	3060	30.6	-4
G-4	[a]32.4	3750	37.5	3340	33.4	+12
	67.0	3620	36.2	4800	48.0	-25
g-4	11.4	2300	23.0	2330	23.3	-1
	32.4	2790	27.9	3270	32.7	-15
	67.0	2670	26.7	3160	31.6	-15
	80.0	2350	23.5	2750	27.5	-15
	105.3	952	9.5	1130	11.3	-16
g-8	11.4	2880	28.8	3300	33.0	-13
	32.4	3710	37.1	4480	44.8	-17
	80.0	3400	34.0	3470	34.7	-2
	105.3	1220	12.2	1550	15.5	-21
g-12	[a]11.4	3350	33.5	3250	32.5	+3
	[a]32.4	4370	43.7	5080	50.8	-14
	[a]67.0	3950	39.5	3050	30.5	+30
	[a]80.0	3250	32.5	4130	41.3	-21
	[a]105.3	1370	13.7	1450	14.5	-6
h-8	[a]11.4	3040	30.4	2180	21.8	+39
	32.4	3750	37.5	4250	42.5	-11
	[a]67.0	3550	35.5	2740	27.4	+30
	80.0	3020	30.2	3700	37.0	-18
	105.3	1260	12.6	1310	13.1	-3
j-4	11.4	2430	24.3	2360	23.6	+3
	32.4	3170	31.7	3640	36.4	-13
	67.0	2880	28.8	3620	36.2	-20
	80.0	2360	23.6	2800	28.0	-16
	105.3	994	9.94	1380	13.8	-28
k-1	11.4	2300	23.0	2290	22.9	+0
	32.4	2920	29.2	3220	32.2	-9
	67.0	2670	26.7	2960	29.6	-7
	105.3	974	9.74	1050	10.5	-7

[a]Suspected defective ionization chamber.

An absolute power level of 84.2 watts was measured. An error of ±7 percent was assigned to this measurement based on the following estimates of individual errors: ±2 percent in the measurement of the subcadmium ratio of gold, ±0.2 percent in the activation cross section of gold, ±4 percent in the calculated conversion factor, and ±5 percent in the measured local to average power distribution.

CONCLUSIONS

The mixed gamma and neutron radiation dose can be measured accurately in a reactor using graphite wall, carbon dioxide filled, and polyethylene wall ethylene filled ionization chambers. The mixed radiation dose can be partitioned to yield separately the value of the gamma and the neutron dose if the ionization chambers are absolutely calibrated both in a pure gamma flux and in the mixed spectrum of a reactor. In the work reported herein, the ionization chambers were absolutely calibrated in a bremsstrahlung spectrum and against a water filled calorimeter in the reactor. In addition, the modest neutron sensitivity of the graphite chambers must be determined. In this work, the neutron sensitivity was calculated.

The agreement between the ATHENA calculated and the measured gamma dose was excellent with a deviation within 10 percent in 10 out of the 16 locations compared. The absolute calculated neutron dose was uniformly low with a deviation from the measurement between -11 percent to -28 percent in 15 out of the 23 locations compared. The cause of this underestimation is not known but may be due to the refined first collision approach used in the calculation. The calculated combined total gamma and neutron dose underestimated the measurement by less than 17 percent in 17 out of the 23 locations investigated.

Lewis Research Center,
National Aeronautics and Space Administration,
Cleveland, Ohio, June 22, 1967,
120-27-06-18-22.

APPENDIX - SYMBOLS

$A(\vec{r})$	normalizing factor relating average dose at $\vec{r}$ to average core dose
B	irradiation dose level of bremsstrahlung beam
C	heat deposition in water mass of calorimeter rad; J/kg
D	dose, rad; J/kg
D_{H_2O}/D_C	ratio of gamma dose deposited in water to gamma dose in graphite
$D_{tot}(\vec{r})$	total dose deposited in 1 gram of material per unit time from fast neutrons at position $\vec{r}$, rad; J/kg
E	energy, eV
ΔE	energy interval, eV
E_i	energy at midpoint of each interval, eV
E_l	lower energy limit of fast neutron range
$F_A(z)$	axial factor corresponding to power at distance z above core bottom plate
$F_R(r)$	radial factor corresponding to relative power density at radius R
f	average fraction of energy imparted to recoiling atom per elastic collision with neutron equal to $2M/(M + 1)^2$
G	gamma dose deposited in water at position of measurement, rad; J/kg
K	ratio of gamma dose in graphite to gamma dose in water; also, gamma dose coefficient or dose reading of graphite chamber per rad (J/kg) gamma dose in water
M	atomic mass
N	fast neutron dose deposited to water at position of measurement, rad; J/kg
ΔN	uncertainty in neutron dose
$\mathcal{N}_i$	number density of i^{th} isotope, atoms/g
n	neutron
R_C	graphite chamber reading for mixed radiation dose of G rad gamma dose plus N rad neutron dose in water, rad; J/kg
R_p	polyethylene chamber reading for mixed radiation dose of G rad; J/kg gamma dose plus N rad neutron dose measured in water, rad; J/kg
r	radius

$\vec{r}$	position vector
S	spectrum index $G/(G + N)$
u	lethargy
Δu	lethargy width equal to 0.1 from 14.9 MeV to 86.5 keV and 0.25 from 86.5 keV to E_L
z	coordinate
δ	neutron dose coefficient or dose reading of polyethylene chamber per rad (J/kg) neutron dose in water
ϵ	gamma response coefficient or dose reading of polyethylene chamber per rad (J/kg) gamma dose in water
ν	ratio of fast neutron dose (rads or J/kg) in carbon dioxide to fast neutron dose (rads or J/kg) in water; dose reading of graphite chamber per rad gamma dose in water or neutron response coefficient
σ_s	elastic scattering cross section, b; m^2
$\varphi(E)$	flux per unit energy interval about energy E
$\varphi(E, \vec{r})$	neutron flux per unit energy about energy E at position $\vec{r}$
$\varphi(U)$	neutron flux per unit lethargy

Subscripts:

C	carbon or graphite
CO_2	carbon dioxide
H	hydrogen
H_2O	water
i	fine group
j	fine group
o	oxygen
'	in LINAC calibration
''	in TRIGA reactor

REFERENCES

1. Bardes, R. G.; et al.: Tungsten Nuclear Rocket, Phase I, Part I. Rep. No. GA-6890 (NASA CR-54909), General Dynamics Corp., Apr. 22, 1966.

2. Houghton, G.; Jupiter, C.; and Trimble, G.: Gamma and Neutron Dose Measurements for a Thermal Tungsten Nuclear Rocket Critical Experiment. Rep. No. GA-6942 (NASA CR-72081), General Dynamics Corp., 1966.

3. Spielberg, D.: ATHENA: A System of FORTRAN Programs for Radiation Transport and Heating Calculations in Complex Reactor Geometries. Rep. No. UNC-5148 (NASA CR-54905), United Nuclear Corp., Mar. 1966.

4. Celnik, J.; and Spielberg, D.: Gamma Spectral Data for Shielding and Heating Calculations. Rep. No. UNC-5140 (NASA CR-54794), United Nuclear Corp., NASA CR-54794, Nov. 30, 1965.

5. Hatcher, C. R.; and Jupiter, C. P.: Measurement of High-Intensity Gamma Radiation. Rep. No. UCRL-7223, University of California Lawrence Radiation Lab., Jan. 31, 1963.

6. Hine, Gerald J.; and Brownell, Gordon L., eds.: Radiation Dosimetry. Academic Press, Inc., 1956, p. 670.

7. Joanou, G. D.; and Dudek, J. S.: GAM-II. A B_3 Code for the Calculation of Fast-Neutron Spectra and Associated Multigroup Constants. Rep. No. GA-4265, General Dynamics Corp., Sept. 16, 1963.

8. Barber, Clayton E.: A Fortran IV Two-Dimensional Discrete Angular Segmentation Transport Program. NASA TN D-3573, 1966.

9. Dorsey, J. P.; Cyl-Champlin, C.; and Kaestner, P. C.: GAMBLE. A Program for the Solution of the Multigroup Neutron-Diffusion Equations in Two Dimensions, with Arbitrary Group Scattering, for the IBM-7090 FORTRAN II System. Rep. No. GA-4246, General Dynamics Corp., June 15, 1963.

NASA-Langley, 1967 —— 22 E-3821

"The aeronautical and space activities of the United States shall be conducted so as to contribute . . . to the expansion of human knowledge of phenomena in the atmosphere and space. The Administration shall provide for the widest practicable and appropriate dissemination of information concerning its activities and the results thereof."

—NATIONAL AERONAUTICS AND SPACE ACT OF 1958

NASA SCIENTIFIC AND TECHNICAL PUBLICATIONS

TECHNICAL REPORTS: Scientific and technical information considered important, complete, and a lasting contribution to existing knowledge.

TECHNICAL NOTES: Information less broad in scope but nevertheless of importance as a contribution to existing knowledge.

TECHNICAL MEMORANDUMS: Information receiving limited distribution because of preliminary data, security classification, or other reasons.

CONTRACTOR REPORTS: Scientific and technical information generated under a NASA contract or grant and considered an important contribution to existing knowledge.

TECHNICAL TRANSLATIONS: Information published in a foreign language considered to merit NASA distribution in English.

SPECIAL PUBLICATIONS: Information derived from or of value to NASA activities. Publications include conference proceedings, monographs, data compilations, handbooks, sourcebooks, and special bibliographies.

TECHNOLOGY UTILIZATION PUBLICATIONS: Information on technology used by NASA that may be of particular interest in commercial and other non-aerospace applications. Publications include Tech Briefs, Technology Utilization Reports and Notes, and Technology Surveys.

Details on the availability of these publications may be obtained from:

SCIENTIFIC AND TECHNICAL INFORMATION DIVISION

NATIONAL AERONAUTICS AND SPACE ADMINISTRATION

Washington, D.C. 20546